

Superintegrability and choreographic obstructions in dihedral n -body Hamiltonian systems

A. M. Escobar-Ruiz^{1*} and M. Fernandez-Guasti¹

^{1*}Departamento de Física, Universidad Autónoma Metropolitana -
Iztapalapa, Rafael Atlixco 186, CDMX, 09340, Ciudad de México,
México.

*Corresponding author(s). E-mail(s): admau@xanum.uam.mx;
Contributing authors: mfg@xanum.uam.mx;

Abstract

We analyze planar n -body Hamiltonian systems with quadratic D_n -invariant interactions and identify the symmetry obstruction to choreographic motion. Choreographies are taken throughout to be collision-free solutions of the equations of motion in which all bodies traverse one closed curve with uniform time shifts. By diagonalizing the dynamics into discrete Fourier sectors, we show that superintegrability, periodicity, and choreography are governed by distinct conditions: commensurability of the active frequencies closes bounded motions, whereas a sectorwise C_n phase-matching condition is required for full equivariance. At the configuration level this equivariance is already equivalent to a genuine simple choreography. Thus generic resonant multi-sector motions are periodic but multi-trace, while true choreographies occur only on phase-matched loci, in single irreducible sectors, or through effective one-sector reductions produced by exact degeneracy. The cases $n = 4, 5, 6$ exhibit this mechanism explicitly, with $n = 6$ marking the first distinction between nondegenerate commensurability and additional exact degeneracy.

Keywords: n -body system, choreography, Hamiltonian system, superintegrability, dynamical fragmentation, first integrals, separation of variables, dihedral group.

1 Introduction

Choreographic solutions of the n -body problem—periodic motions in which identical particles traverse the same closed curve with uniform time delays—occupy a central place in the modern theory of Hamiltonian dynamics [1–12]. In the classical gravitational problem and related nonintegrable settings, such motions are typically found through variational, topological, or numerical methods [1–3, 7, 13–16], and are therefore known more often through special constructions than through explicit symmetry-adapted analytic descriptions [17]. Related symmetry-driven developments include the study of symmetric central configurations and extensions of the n -body problem to spaces of constant curvature [18, 19]. This suggests a basic question: when does periodic motion realize choreography as a genuine space-time symmetry, and when does it fail to do so?

In this work we address that question in a class of exactly solvable planar n -body Hamiltonian systems with quadratic pairwise interactions whose coupling pattern is invariant under the dihedral group D_n . These systems are simple enough to admit an exact Fourier normal-mode decomposition, yet rich enough to display nontrivial choreographic behavior. The present approach is complementary to variational existence theory, numerical construction, and central-configuration geometry: we exploit the explicit Fourier-sector decomposition of quadratic D_n -invariant Hamiltonians to disentangle superintegrability, periodicity, equivariance, and choreography.

Throughout this paper, an *n -body choreography* means a collision-free periodic solution of the equations of motion in which all particle positions $\mathbf{r}_i(t) \in \mathbb{R}^2$ are time shifts of one and the same closed curve $\gamma(t)$,

$$\mathbf{r}_j(t) = \mathbf{r}_1\left(t + \frac{j-1}{n}T\right), \quad j = 1, \dots, n, \quad T > 0.$$

Collision-freeness is imposed as a standing admissibility condition: throughout the motion,

$$\mathbf{r}_i(t) \neq \mathbf{r}_j(t), \quad i \neq j,$$

and collisional trajectories are not considered in this work. Every n -body choreographic motion is invariant under the choreography generator, namely the combined action of a time shift by T/n and cyclic relabeling of the particles. We refer to this symmetry property as full C_n -equivariance. In the present full-configuration formulation, Corollary 1 shows that full C_n -equivariance already yields the simple (single-trace) choreography relation. The relevant distinction is therefore not between full C_n -equivariance and single-trace choreography, but between full C_n -equivariance and weaker periodic multi-trace motions. When the particles decompose into synchronized subsets, each subset tracing its own closed curve with uniform time shifts, the resulting configuration is called *choreographic fragmentation*, or equivalently *multiple choreographies* in the terminology of [11].

Why quadratic D_n models? The present work examines a class of analytically transparent planar n -body Hamiltonians with pairwise quadratic interactions $V = V(|\mathbf{r}_i - \mathbf{r}_j|^2)$ whose *index couplings* are invariant under the dihedral group D_n , i.e., under the symmetry of the edges and diagonals of the abstract n -gon. Here

D_n -invariance refers to the interaction pattern on labeled particles, not to the instantaneous geometric shape of the configuration. These models are useful because three structural features coexist in closed form: the internal dynamics diagonalizes exactly under a discrete Fourier transform; the normal modes organize into symmetry-adapted irreducible D_n sectors, together with the modal degeneracies imposed by dihedral symmetry; and, for suitable rational relations among the active frequencies Ω_ℓ , the system becomes maximally superintegrable, so that all bounded motions are closed and explicitly solvable [20–23]. This framework also separates degeneracies forced by symmetry from additional exact spectral coincidences that may arise at special parameter values. The central point is that commensurability alone does *not* guarantee an n -body choreography: periodicity is a spectral statement, whereas choreography requires the cyclic symmetry to be realized through a combined space-time operation. In Fourier language, each dynamically active sector must acquire, under the time shift T/n , exactly the character phase prescribed by its C_n label, and this is the content of Theorem 2. The obstruction to choreography is therefore representation-theoretic, not merely spectral. Equivalently, the dihedral symmetry both organizes the internal dynamics into symmetry-adapted sectors and fixes the modal degeneracies forced by symmetry, while the cyclic subgroup C_n acts on each sector through a definite character. This sharpens the distinction between *algebraic resonances*, which ensure periodicity, and *choreographic resonances*, which in addition satisfy the phase-matching condition of Theorem 2; it also clarifies the difference between degeneracies imposed by D_n itself and additional exact spectral coincidences. In this sense, the present analysis complements recent work connecting choreographies with additional *particular* integrals of motion [24–26]. For a comprehensive presentation of the structure and characters of the irreducible representations of the dihedral group, we refer the reader to [27–29].

In the full-configuration setting adopted here, and within the collision-free class considered throughout, the symmetry condition of Theorem 2 has a direct geometric consequence: by Corollary 1, full C_n -equivariance already implies a genuine simple, single-trace choreography. Collisional trajectories are excluded by assumption and are not analyzed in this work. The relevant distinction is therefore not between full C_n -equivariance and single-trace choreography, but between full C_n -equivariance and periodic multi-trace motion. Generic simultaneous excitation of inequivalent sectors obstructs full equivariance and instead produces periodic multi-trace motion. Genuine choreographies nevertheless arise from a single irreducible sector, from a specially phase-matched multi-sector resonance, or from an effective one-sector structure produced by additional exact degeneracy. In structured cases, the resulting multi-trace splitting organizes into synchronized sub-choreographies on distinct closed curves, giving rise to choreographic fragmentation; see Table 1.

The low-dimensional cases already exhibit the core mechanism. For $n = 4$ and $n = 5$, only two inequivalent internal sectors occur, and the corresponding choreographic families reduce, up to symmetry, to limaçon-type deformations [24, 30, 31]. The first genuinely new case is $n = 6$, where three inequivalent sectors coexist. The novelty there is not a failure of full equivariance to imply choreography, but the emergence of a richer resonance structure: two independent resonance ratios, a broader family of

| Active sectors | Frequency relations | D_n content | Resulting motion |
|---------------------------------------|------------------------------------|--|---|
| Single sector (or effectively single) | One frequency or exact degeneracy | One 2D doublet (or an effective sector via degeneracy) | Full C_n -equivariance; single-trace choreography |
| Multiple inequivalent sectors | Commensurate and phase matched | Inequivalent irreps | D_n Special multi-sector C_n -equivariant motion; genuine single-trace choreography |
| Multiple inequivalent sectors | Commensurate but not phase matched | Inequivalent irreps | D_n Periodic motion; generically not fully C_n -equivariant; often multi-trace; fragmentation in structured cases |
| Multiple inequivalent sectors | Incommensurate | Inequivalent irreps | D_n Quasiperiodic (non-closed) motion |

Table 1 Quadratic D_n -invariant n -body dynamics: commensurability \Rightarrow periodicity, while sectorwise phase matching [Theorem 2] selects the C_n -equivariant periodic motions. In the full-configuration setting, C_n -equivariance implies a genuine single-trace choreography.

periodic multi-trace motions with reduced symmetry, and a sharp distinction between nondegenerate commensurability and additional exact degeneracy. In particular, $1:2:3$ is a nondegenerate resonance among three distinct frequency branches, whereas $1:2:2$ is distinguished by the further exact degeneracy $\Omega_2 = \Omega_3$, which can support an effective one-sector description only under the appropriate phase-locking or invariant-subspace constraints. Figure 1 summarizes the structural logic of the paper.

It is also useful to distinguish the present viewpoint from inverse-design approaches such as Ref. [31], where one prescribes a target curve and reconstructs couplings that realize it. Here the logic is the opposite: the couplings are fixed *a priori* by the imposed quadratic form of the potential, and the D_n active Fourier sectors determine which choreographic or fragmented motions can occur. The advantage of this forward, symmetry-constrained perspective is that the admissible dynamical patterns follow directly from the representation-theoretic structure of the model.

The paper is organized as follows. Section 2 develops the symmetry-adapted Fourier description of the internal dynamics and proves Theorem 2, our criterion for C_n -equivariance. Section 3 draws its main consequences for periodicity, equivariance, and the emergence of multi-trace motion. Sections 4 and 5 analyze explicitly the cases $n = 4, 5, 6$, highlighting the emergence of choreographic fragmentation at $n = 6$. Section 6 isolates the geometric mechanism behind fragmentation, and Section 7 summarizes the main findings.

2 D_n -invariant Hamiltonian and the phase-matching criterion

This section sets the symmetry-adapted framework for choreographic motion in quadratic D_n -invariant n -body systems. Exact separability emerges due to the quadratic nature of the potential, but the key structural fact is that the D_n symmetry organizes the internal dynamics exactly into $\lfloor n/2 \rfloor$ Fourier sectors, while the choreography symmetry acts on each sector through a fixed character of C_n . This leads to a

Quadratic D_n systems: superintegrability, phase matching, and choreography

Symmetry-resolved organization of collision-free choreographic dynamics

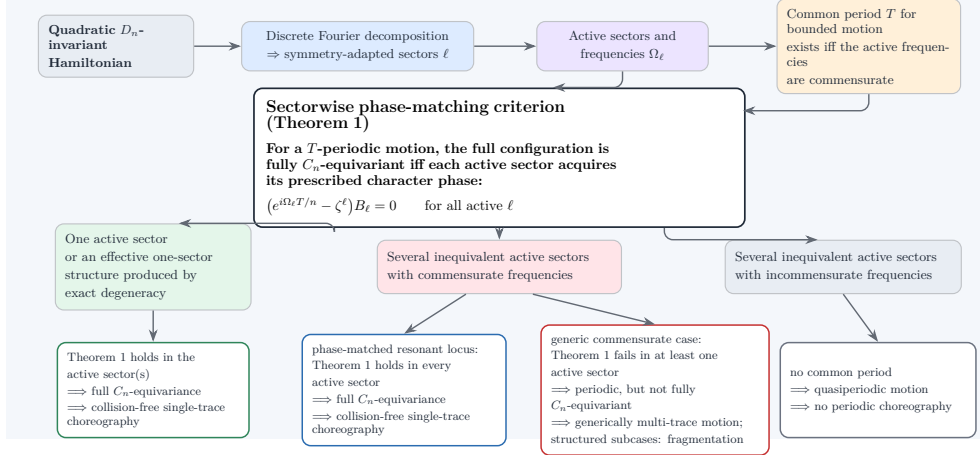


Fig. 1 Symmetry-resolved organization of quadratic D_n -invariant n -body dynamics. Commensurability of the active frequencies controls periodicity, while the sectorwise phase-matching condition of Theorem 2 controls full C_n -equivariance. Within the collision-free class considered throughout, full C_n -equivariance implies a genuine single-trace choreography; failure of phase matching gives periodic but non-equivariant motion, generically multi-trace, with choreographic fragmentation occurring in structured subcases.

precise criterion for C_n -equivariance of periodic motions, which is the theorem needed for the rest of the paper.

2.1 Choreographies, equivariance, and traces

Consider n identical particles moving on the plane, with positions $\mathbf{r}_i(t) \in \mathbb{R}^2$, $i = 1, \dots, n$, satisfying the equations of motion and remaining collision-free on their interval of definition. A *simple (single-trace) n -body choreography* is a periodic solution of period $T > 0$ for which there exists a generating curve $\gamma(t)$ such that

$$\mathbf{r}_i(t) = \gamma\left(t + \frac{(i-1)T}{n}\right), \quad i = 1, \dots, n. \quad (1)$$

No geometric n -fold symmetry of γ is assumed. Every such motion is invariant under the choreography generator

$$t \mapsto t + \frac{T}{n}, \quad i \mapsto i + 1 \pmod{n},$$

and we refer to this symmetry as C_n -equivariance.

Writing $\mathbf{R}(t) := (\mathbf{r}_1(t), \dots, \mathbf{r}_n(t))$, we distinguish three notions: (i) *periodicity*, $\mathbf{R}(t+T) = \mathbf{R}(t)$; (ii) *full C_n -equivariance*, invariance under cyclic relabeling combined

with the time shift T/n ; and (iii) *structured multi-trace periodic motion*, in which the particles split into synchronized subsets supported on distinct closed curves. In the present full-configuration setting, full C_n -equivariance is stronger than periodicity and, by Theorem 2 together with Corollary 1, already implies the uniform-delay choreography relation (1). The relevant distinction below is therefore not between full C_n -equivariance and single-trace choreography, but between full C_n -equivariance and weaker periodic or resonant motions, including fragmented motions or choreographies visible only after restriction to a proper invariant subspace.

2.2 D_n -invariant quadratic systems and Fourier sectors

We consider the quadratic Hamiltonian

$$\mathcal{H}_n = \frac{1}{2\mu} \sum_{i=1}^n \mathbf{p}_i^2 + \frac{1}{2} \mu \omega^2 \sum_{k=1}^{\lfloor n/2 \rfloor} \kappa_k^{(n)} \sum_{i=1}^n (\mathbf{r}_i - \mathbf{r}_{i+k})^2, \quad (2)$$

which is invariant under the dihedral group D_n acting on particle labels. Here $\mu > 0$ is the common mass, $\omega > 0$, and the real parameters $\kappa_k^{(n)}$ are coupling constants.

Remark 1 (Normalization for even n) For even n , the term with $k = n/2$ corresponds to opposite vertices. In the double sum

$$\sum_{k=1}^{\lfloor n/2 \rfloor} \sum_{i=1}^n (\mathbf{r}_i - \mathbf{r}_{i+k})^2,$$

these opposite bonds are counted twice. Throughout the paper we adopt this uniform convention for all n . If one instead counts opposite bonds only once, as is common for $n = 4$, the corresponding coupling must be rescaled by a factor of 2, i.e. $\kappa_{n/2}^{(n)} \mapsto 2\kappa_{n/2}^{(n)}$.

Passing to the center-of-mass frame,

$$\sum_{i=1}^n \mathbf{r}_i = \sum_{i=1}^n \mathbf{p}_i = 0,$$

the quadratic form becomes circulant in the particle labels and is therefore diagonalized by the discrete Fourier transform. In real Cartesian vector notation,

$$\mathbf{r}_i = \frac{1}{\sqrt{n}} \sum_{\ell=0}^{n-1} \mathbf{U}_\ell e^{2\pi i \ell(i-1)/n}, \quad \mathbf{U}_{n-\ell} = \overline{\mathbf{U}_\ell},$$

where $\mathbf{r}_i \in \mathbb{R}^2$, $\mathbf{U}_\ell \in \mathbb{C}^2$, and the conjugation is understood componentwise. Thus the internal dynamics decomposes into D_n -invariant Fourier sectors indexed by ℓ . For $\ell \neq 0, n/2$, the pair $(\ell, n-\ell)$ spans one real cosine-sine sector in label space, tensored with

the physical plane; for even n , the Nyquist sector $\ell = n/2$ is self-conjugate and one-dimensional in label space. Hence the internal motion is a superposition of uncoupled sectoral oscillators, each associated with a definite irreducible representation of D_n .

2.3 Normal-mode decomposition

Proposition 1 (Normal-mode decomposition) *Consider the planar quadratic n -body Hamiltonian (2) in the center-of-mass frame, and assume its quadratic interaction is D_n -invariant in the particle labels. Then the internal quadratic form in label space is represented by a real symmetric circulant matrix. Consequently, the discrete Fourier transform diagonalizes the internal Hamiltonian and decomposes the motion into D_n -invariant Fourier sectors indexed by*

$$\ell \in \{0, 1, \dots, \lfloor n/2 \rfloor\}.$$

For each nontrivial sector ℓ , the equations of motion reduce to an uncoupled harmonic mode with frequency Ω_ℓ ; equivalently, for $\ell \neq 0, n/2$, the conjugate pair $(\ell, n - \ell)$ forms one real two-dimensional cosine-sine sector with common frequency Ω_ℓ , while for even n the Nyquist sector $\ell = n/2$ is one-dimensional. Hence every solution is a superposition of sectoral modes, and the set of active sectors is determined by the initial data.

Proof Because the Hamiltonian is quadratic and the masses are equal, the kinetic term is already diagonal in particle-label space, up to the removal of the center-of-mass mode. The interaction is D_n -invariant on the labels, so its stiffness matrix commutes with the cyclic shift and is therefore circulant. Since the interaction is quadratic, this matrix is also real symmetric. Every real symmetric circulant matrix is diagonalized by the discrete Fourier transform. Applying the same Fourier change of variables to coordinates and momenta gives a canonical transformation, so the internal Hamiltonian splits into independent normal modes labeled by ℓ .

The Fourier modes furnish invariant subspaces for the D_n -action. For $\ell \neq 0, n/2$, the pair $(\ell, n - \ell)$ combines into one real two-dimensional cosine-sine sector; for even n , the Nyquist mode $\ell = n/2$ is self-conjugate and one-dimensional. In each sector the equations reduce to an uncoupled oscillator with frequency Ω_ℓ , determined by the corresponding eigenvalue of the stiffness matrix. Therefore the full internal motion is the superposition of these sectoral oscillations, and the active sectors are exactly those whose amplitudes are selected as nonzero by the initial data. \square

2.4 Phase-matching and C_n -equivariance

To formulate the C_n -equivariance condition, we identify the plane with $\mathbb{C} \simeq \mathbb{R}^2$ and regard the configuration as an element of \mathbb{C}^n ,

$$R(t) := (r_1(t), \dots, r_n(t)) \in \mathbb{C}^n.$$

Let

$$\zeta := e^{2\pi i/n},$$

and define the discrete Fourier coefficients in the particle label by

$$U_\ell(t) := \frac{1}{\sqrt{n}} \sum_{j=1}^n r_j(t) \zeta^{-\ell(j-1)}, \quad \ell = 0, 1, \dots, n-1. \quad (3)$$

The inverse transform is

$$r_i(t) = \frac{1}{\sqrt{n}} \sum_{\ell=0}^{n-1} U_\ell(t) \zeta^{\ell(i-1)}, \quad i = 1, \dots, n. \quad (4)$$

In the center-of-mass frame $U_0 \equiv 0$. Since the planar coordinates have already been identified with complex numbers, no componentwise reality condition such as $U_{n-\ell} = \overline{U_\ell}$ is imposed on these complex Fourier coefficients. Rather, for $\ell \neq 0, n/2$, the pair of label characters $(\ell, n-\ell)$ spans the corresponding real cosine-sine sector in label space; for even n , the Nyquist mode $\ell = n/2$ is self-conjugate.

For each internal sector $\ell \in \{1, \dots, \lfloor n/2 \rfloor\}$, the sectoral coefficient satisfies an uncoupled oscillator equation

$$\ddot{U}_\ell + \Omega_\ell^2 U_\ell = 0, \quad \Omega_\ell > 0. \quad (5)$$

Let \mathcal{A} denote the set of dynamically active sectors. For the phase-matched families considered below, we use a reduced one-sided notation for each active non-self-conjugate sector:

$$U_\ell(t) = B_\ell e^{i\Omega_\ell t}, \quad B_\ell \in \mathbb{C}, \quad B_\ell \neq 0. \quad (6)$$

This convention describes the circular traveling-wave components relevant for the choreographic ansatz. The corresponding fully real oscillator description, including the cosine-sine normal coordinates, is given in Appendix A.

Let $c : \mathbb{C}^n \rightarrow \mathbb{C}^n$ denote cyclic relabeling,

$$cR := (r_2(t), r_3(t), \dots, r_n(t), r_1(t)),$$

and let

$$v^{(\ell)} := \frac{1}{\sqrt{n}} (1, \zeta^\ell, \zeta^{2\ell}, \dots, \zeta^{(n-1)\ell}) \in \mathbb{C}^n$$

be the ℓ -th Fourier basis vector in label space. Then

$$c v^{(\ell)} = \zeta^\ell v^{(\ell)}.$$

Thus the cyclic generator acts on the ℓ -th label-Fourier sector through the character ζ^ℓ , and C_n -equivariance reduces to a sectorwise phase-matching condition.

Theorem 2 (C_n -equivariance in the traveling-wave Fourier class) *Let*

$$R(t) = (r_1(t), \dots, r_n(t)) \in \mathbb{C}^n$$

be a T -periodic solution of the quadratic D_n -invariant planar n -body system in the center-of-mass frame. Write

$$R(t) = \sum_{\ell=0}^{n-1} U_\ell(t)v^{(\ell)}, \quad v_j^{(\ell)} = \frac{1}{\sqrt{n}}\zeta^{\ell(j-1)}, \quad \zeta = e^{2\pi i/n},$$

so that $cv^{(\ell)} = \zeta^\ell v^{(\ell)}$. Assume that every active non-self-conjugate sector belongs to the one-sided traveling-wave class

$$U_\ell(t) = B_\ell e^{i\Omega_\ell t}, \quad B_\ell \neq 0.$$

For even n , the Nyquist sector $\ell = n/2$, when active, is included with $\zeta^{n/2} = -1$.

Then $R(t)$ is C_n -equivariant,

$$cR(t) = R\left(t + \frac{T}{n}\right),$$

if and only if every active non-self-conjugate sector satisfies

$$(e^{i\Omega_\ell T/n} - \zeta^\ell)B_\ell = 0. \quad (7)$$

If the Nyquist sector is active, the corresponding condition is

$$U_{n/2}\left(t + \frac{T}{n}\right) = -U_{n/2}(t),$$

equivalently

$$e^{i\Omega_{n/2}T/n} = -1 = \zeta^{n/2}.$$

Thus every active traveling-wave sector acquires the character phase ζ^ℓ under the time shift T/n .

Proof Since $cv^{(\ell)} = \zeta^\ell v^{(\ell)}$, the identity

$$cR(t) = R\left(t + \frac{T}{n}\right)$$

is equivalent, after projection onto each active Fourier sector, to

$$\zeta^\ell U_\ell(t) = U_\ell\left(t + \frac{T}{n}\right).$$

For a non-self-conjugate traveling-wave sector,

$$U_\ell(t) = B_\ell e^{i\Omega_\ell t},$$

this becomes

$$\zeta^\ell B_\ell e^{i\Omega_\ell t} = B_\ell e^{i\Omega_\ell(t+T/n)},$$

which is equivalent to

$$(e^{i\Omega_\ell T/n} - \zeta^\ell)B_\ell = 0.$$

For the even- n Nyquist sector, $cv^{(n/2)} = -v^{(n/2)}$, so equivariance is equivalent to

$$U_{n/2}\left(t + \frac{T}{n}\right) = -U_{n/2}(t).$$

This is equivalent to

$$e^{i\Omega_{n/2}T/n} = -1 = \zeta^{n/2}$$

for any nonzero Nyquist oscillator component. Summing over the active sectors gives the result. \square

Corollary 1 *Let*

$$R(t) = (r_1(t), \dots, r_n(t)) \in \mathbb{C}^n$$

be a T -periodic collision-free solution of the equations of motion in the center-of-mass frame. If

$$cR(t) = R\left(t + \frac{T}{n}\right), \quad (cR)_i = r_{i+1} \pmod{n},$$

then

$$r_j(t) = r_1\left(t + \frac{(j-1)T}{n}\right), \quad j = 1, \dots, n.$$

Hence $R(t)$ is a single-trace choreography in the sense of (1), with generating curve $\gamma(t) := r_1(t)$.

Proof The identity

$$cR(t) = R\left(t + \frac{T}{n}\right)$$

is equivalent componentwise to

$$r_{i+1}(t) = r_i\left(t + \frac{T}{n}\right).$$

Iterating this relation gives

$$r_j(t) = r_1\left(t + \frac{(j-1)T}{n}\right), \quad j = 1, \dots, n,$$

which is exactly the defining form (1) of a single-trace choreography. \square

Remark 2 (Meaning of the Fourier coefficient U_ℓ) The quantity $U_\ell(t)$ is not the position of an individual particle; rather, it is the ℓ -th discrete Fourier coefficient of the full configuration $R(t) = (r_1(t), \dots, r_n(t)) \in \mathbb{C}^n$ with respect to the particle label. Equation (4) reconstructs the particle trajectories from the sector coefficients, so the phase-matching condition (7) describes how each active Fourier sector of the configuration transforms under the choreography generator.

Remark 3 (Full equivariance versus periodic multi-trace motion) Theorem 2 characterizes full C_n -equivariance within the traveling-wave Fourier class considered here. By Corollary 1, this already implies the single-trace choreography relation (1). Thus the relevant distinction is not between full C_n -equivariance and single-trace choreography, but between full C_n -equivariance and weaker periodic multi-trace motions arising in reduced ansätze, one-sided families, or proper invariant subspaces. Under simultaneous excitation of inequivalent D_n -sectors, what generically fails is full equivariance itself: the motion may remain periodic and geometrically multi-trace, possibly decomposing into synchronized sub-choreographies on distinct curves, without satisfying the configuration-level condition of Theorem 2.

Remark 4 (Dictionary with the real normal coordinates used in Appendix A) The main text is formulated in terms of the complex label-Fourier coefficients U_ℓ . In Appendix A we instead use real symmetry-adapted normal coordinates, such as s_i , $u_{c\ell}$, and $u_{s\ell}$. These are equivalent descriptions of the same sector decomposition.

For $\ell \neq 0, n/2$, the pair of label characters $(\ell, n - \ell)$ is realized in real coordinates as one cosine-sine doublet

$$(u_{c\ell}, u_{s\ell}).$$

After identifying the plane with \mathbb{C} , this doublet can be encoded by the two complex label-Fourier coefficients U_ℓ and $U_{n-\ell}$, as described explicitly in Appendix A. For even n , the Nyquist sector $\ell = n/2$ is represented by a single real normal coordinate. Thus Appendix A gives the real-coordinate realization of the Fourier-sector decomposition used in Theorem 2.

In practice, for a quadratic D_n -invariant system and a candidate periodic solution in the traveling-wave Fourier class, one first decomposes the internal motion into Fourier normal modes and identifies the active sectors \mathcal{A} . One then computes the corresponding frequencies Ω_ℓ , amplitudes B_ℓ , and a common period T , when the active frequencies are commensurate, and finally tests

$$(e^{i\Omega_\ell T/n} - \zeta^\ell)B_\ell = 0$$

in every active sector.

This leads to three regimes. If commensurability fails, the motion is nonperiodic and choreography is excluded. If commensurability holds but Eq. (7) fails in some active sector, the motion is periodic but not fully C_n -equivariant, hence not a choreography. If Eq. (7) holds in all active sectors, the motion is fully C_n -equivariant and, by Corollary 1, is a genuine single-trace choreography of the full configuration.

The complementary cases—failure of Eq. (7) or restriction to reduced one-sided families, ansätze, or proper invariant subspaces—are where the multi-sector geometry becomes richer: periodic resonant motions may remain multi-trace and organize into choreographic fragmentation. The next proposition makes this generic obstruction precise by showing that, once several inequivalent active sectors are present, single-trace choreography becomes exceptional rather than typical.

Proposition 3 (Generic obstruction to full C_n -equivariance in nondegenerate multi-sector periodic families) *Assume $n \geq 6$, and let $\{R_\lambda(t)\}_{\lambda \in M}$ be a real-analytic family of $T(\lambda)$ -periodic solutions of the quadratic D_n -invariant system, parametrized by a real-analytic manifold M . Suppose that, throughout the family, the active sectors are non-self-conjugate and admit the one-sided form*

$$U_\ell(t; \lambda) = B_\ell(\lambda)e^{i\Omega_\ell(\lambda)t}, \quad \ell \in \mathcal{A},$$

with a fixed active set

$$\mathcal{A} \subset \{1, \dots, \lfloor n/2 \rfloor\}$$

containing at least two inequivalent sectors, and assume that no exact spectral degeneracy collapses these active sectors into a single effective irreducible sector. Let

$$M^* := \{\lambda \in M : B_\ell(\lambda) \neq 0 \text{ for all } \ell \in \mathcal{A}\}.$$

If $M^* \neq \emptyset$ and the phase-matching identities

$$e^{i\Omega_\ell(\lambda)T(\lambda)/n} = \zeta^\ell, \quad \ell \in \mathcal{A},$$

do not hold identically on M^* , then the set of parameters for which $R_\lambda(t)$ is fully C_n -equivariant is contained in a proper real-analytic subset of M^* . In particular, full C_n -equivariance is nongeneric in the family: for generic $\lambda \in M^*$, the periodic motion $R_\lambda(t)$ is not fully C_n -equivariant, and therefore is not a single-trace choreography.

Proof By Theorem 2, $R_\lambda(t)$ is fully C_n -equivariant if and only if

$$(e^{i\Omega_\ell(\lambda)T(\lambda)/n} - \zeta^\ell)B_\ell(\lambda) = 0, \quad \ell \in \mathcal{A}.$$

On M^* all amplitudes $B_\ell(\lambda)$ are nonzero, so this is equivalent to

$$e^{i\Omega_\ell(\lambda)T(\lambda)/n} = \zeta^\ell, \quad \ell \in \mathcal{A}.$$

Thus the equivariant locus in M^* is the common zero set of the real-analytic functions

$$f_\ell(\lambda) := e^{i\Omega_\ell(\lambda)T(\lambda)/n} - \zeta^\ell, \quad \ell \in \mathcal{A}.$$

If these identities do not hold identically on M^* , then at least one f_ℓ is not identically zero, and its zero set is a proper real-analytic subset of M^* . Hence the simultaneous phase-matching locus is also contained in a proper real-analytic subset of M^* .

Therefore, for generic $\lambda \in M^*$, the phase-matching condition fails in at least one active inequivalent sector, so $R_\lambda(t)$ is not fully C_n -equivariant. Corollary 1 then implies that it cannot be a single-trace choreography. \square

3 Consequences of the phase-matching criterion

Theorem 2 isolates the symmetry requirement for choreographic motion in quadratic D_n -invariant systems. Its first consequence is immediate: failure of the sectorwise phase-matching condition rules out C_n -equivariance, and therefore rules out single-trace choreography.

Lemma 1 (Obstruction to C_n -equivariance (and hence choreography)) Let $R(t)$ be a T -periodic solution in the traveling-wave Fourier class of Theorem 2, and let \mathcal{A} denote the active Fourier sectors. If the phase-matching condition (7) fails for at least one active sector, then $R(t)$ is not C_n -equivariant. In particular, $R(t)$ cannot be a single-trace choreography.

Proof By Theorem 2, the motion $\mathbf{R}(t)$ is C_n -equivariant if and only if

$$c\mathbf{R}(t) = \mathbf{R}\left(t + \frac{T}{n}\right),$$

or equivalently if and only if the sectorwise phase-matching condition (7) holds in every active Fourier sector.

If (7) fails for some $\ell \in \mathcal{A}$, then the ℓ th sector does not transform correctly under the combined action of the time shift $t \mapsto t + T/n$ and the cyclic relabeling c . Hence

$$c\mathbf{R}(t) \neq \mathbf{R}\left(t + \frac{T}{n}\right),$$

so $\mathbf{R}(t)$ is not C_n -equivariant.

Finally, every single-trace choreography is, in particular, C_n -equivariant. Therefore $\mathbf{R}(t)$ cannot be a choreography. \square

3.1 Superintegrability, periodicity, equivariance, and fragmentation

For a Hamiltonian system with d degrees of freedom, maximal superintegrability means the existence of $2d - 1$ functionally independent conserved quantities, including the Hamiltonian. In the present setting its main dynamical consequence is that bounded motions are periodic precisely when the *active* normal-mode frequencies are rationally commensurate, i.e. when there exist $\Omega_0 > 0$ and integers $m_\ell \in \mathbb{Z}$ such that

$$\Omega_\ell = m_\ell \Omega_0 \quad \text{for every active sector } \ell.$$

This condition is purely spectral. By contrast, C_n -equivariance imposes an additional representation-theoretic requirement: by Theorem 2, each nonzero active sector must acquire under the time shift $\tau_n := T/n$ the character phase $\zeta^\ell = e^{2\pi i \ell/n}$. Thus commensurability guarantees periodicity, but phase matching decides whether the resulting periodic orbit realizes the cyclic space-time symmetry.

Equation (7) is sectorwise: it depends on which sectors are active, and for each nonzero active sector it constrains the relation between Ω_ℓ and the common period T . Accordingly, commensurability is necessary but not sufficient for choreography. A motion may be periodic and still fail the phase-matching condition, in which case it is not fully C_n -equivariant and therefore cannot be a choreography. In the present full-configuration setting, however, full C_n -equivariance already implies a genuine single-trace choreography by Corollary 1. The relevant geometric distinction is therefore not between equivariance and single-trace choreography, but between full C_n -equivariance and periodic multi-trace motion.

In special cases, multi-trace motion organizes into synchronized subsets of particles, each subset traversing its own closed curve with uniform time shifts. Such subsets form sub-choreographies; when they are supported on distinct closed curves, we refer to the resulting structured splitting as *choreographic fragmentation*. Schematically,

$$\text{commensurability of active frequencies} \implies \text{periodicity,}$$

while

$$\text{periodicity+phase matching (7)} \implies \text{full } C_n\text{-equivariance} \implies \text{single-trace choreography,}$$

whereas

$$\text{periodicity + failure of (7)} \implies \text{not fully } C_n\text{-equivariant,}$$

with the resulting motion often multi-trace or fragmented, sometimes only after restriction to a reduced invariant subspace. The remainder of the paper illustrates this mechanism in concrete examples: Section 4 treats the low- n cases $n = 4$ and $n = 5$, while Section 5 treats the six-body problem, where the first genuinely exact degeneracy structure appears. In this work, fragmentation is used as a structural description of organized multi-trace periodic motion, not as a complete classification of all admissible splittings.

4 Low- n illustrations: four and five bodies

We now illustrate the framework of Sections 2 and 3 in the simplest nontrivial cases $n = 4$ and $n = 5$. In both, only two inequivalent internal frequency branches occur, which makes the geometry especially transparent. Unless stated otherwise, however, the explicit “choreographic resonances” discussed below should be understood as belonging to one-sided families, reduced invariant subspaces, or effective one-sector regimes created by exact degeneracy, rather than as generic full-phase-space consequences of frequency commensurability alone; the relevant realizations are given in Appendix A.

4.1 Case $n = 4$

Section 4.1 is devoted to the case $n = 4$, which already illustrates the separation between (i) periodicity, controlled by commensurability of the internal frequencies, (ii) C_4 -equivariance, controlled by the phase-matching constraint of Theorem 2, and (iii) the geometric distinction between a single four-body choreography (one common trace) and choreographic fragmentation (multiple traces), which depends on which D_4 sectors are dynamically active. In this case the internal spectrum consists of one 2D D_4 doublet and one 1D Nyquist sector, so at most two frequency branches can appear, but a four-body choreography need not involve both.

4.2 Hamiltonian and D_4 -invariant potential

First, let us consider the classical system of four particles moving in the Euclidean plane \mathbb{R}^2 , with equal masses ($m_1 = m_2 = m_3 = m_4 = \mu$) and subject to a quadratic pairwise interaction potential. The corresponding Hamiltonian is

$$\mathcal{H}_4 = \frac{1}{2\mu}(\mathbf{p}_1^2 + \mathbf{p}_2^2 + \mathbf{p}_3^2 + \mathbf{p}_4^2) + V_4(r_{ij}), \quad (8)$$

where the potential takes the D_4 -invariant form

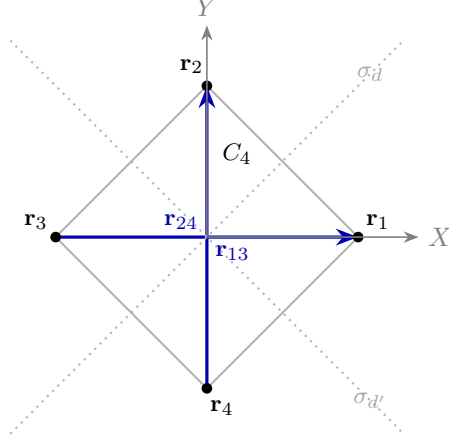
$$V_4(r_{ij}) = \frac{1}{2}\mu\omega^2 \left[\kappa_1^{(4)} (r_{12}^2 + r_{23}^2 + r_{34}^2 + r_{14}^2) + \kappa_2^{(4)} (r_{13}^2 + r_{24}^2) \right]. \quad (9)$$

We fix the coupling constants to

$$\kappa_1^{(4)} = 1 > 0, \quad \kappa_2^{(4)} = -\frac{1}{2} < 0. \quad (10)$$

This particular choice (10) has appeared previously and was studied in detail in [24]. As usual, $\mathbf{r}_{ij} = \mathbf{r}_i - \mathbf{r}_j$ denotes the relative position vector between particles i and j , and $r_{ij} = |\mathbf{r}_{ij}|$ its magnitude (the relative distance). The phase space has dimension 16. Nearest-neighbor interactions carry strength $\frac{1}{2}\mu\omega^2$, while opposite vertices interact with half that strength and with opposite (repulsive) sign. Details of the separation of variables and the resulting trajectories are given in Appendix A.1.

Figure 2 illustrates the D_4 symmetry at $n = 4$ in terms of distinguished relative coordinates: the dihedral action on the labels is generated by the cyclic relabeling C_4



$$D_4 = \langle C_4, \sigma_X \rangle$$

Fig. 2 Distinguished relative coordinates and the action of D_4 for $n = 4$. Here σ_d denotes reflections across axial and diagonal mirror axes of the square, respectively.

together with an axial reflection (and hence also the diagonal reflections), and here D_4 -invariance refers to the symmetry of the *index couplings* (edges/diagonals of the abstract square), not necessarily to an instantaneous square configuration. Visually, basic subgroups correspond to rigid symmetries of the coupling pattern (e.g. the half-turn $C_2 \leq C_4$ pairs opposite vertices, while reflections pair vertices across a mirror axis), and these orbit partitions anticipate the possible ways bodies can organize into synchronized groups when more than one sector is active.

4.3 General frequencies, superintegrability, and choreographies

For the quadratic four-body potential (9) with arbitrary couplings $(\kappa_1^{(4)}, \kappa_2^{(4)})$, diagonalization of the Hamiltonian (8) yields one zero center-of-mass mode, $\Omega_0 = 0$, and three internal frequencies

$$\Omega_1 = 2\omega\sqrt{\kappa_1^{(4)}}, \quad \Omega_2 = \Omega_3 = \omega\sqrt{2(\kappa_1^{(4)} + \kappa_2^{(4)})}.$$

Assuming $\kappa_1^{(4)} > 0$, $\kappa_1^{(4)} + \kappa_2^{(4)} > 0$, and $2\kappa_1^{(4)} > \kappa_1^{(4)} + \kappa_2^{(4)}$, the lower branch is the doubly degenerate one,

$$\Omega_F := \Omega_2 = \Omega_3, \quad \Omega_N := \Omega_1, \quad \frac{\Omega_N}{\Omega_F} = \sqrt{\frac{2\kappa_1^{(4)}}{\kappa_1^{(4)} + \kappa_2^{(4)}}}.$$

Thus the internal dynamics consists of a 2D D_4 doublet with frequency Ω_F and a 1D Nyquist sector with frequency Ω_N . If both sectors are active, periodicity requires $\Omega_N/\Omega_F \in \mathbb{Q}$, but choreography requires in addition the C_4 phase-matching condition.

If the Nyquist sector is inactive, the problem reduces to phase locking within the D_4 doublet, leading generically to a synchronized $(2 + 2)$ dimer motion and, for special relative phases, to a single four-body trace; see Section 4.3.1.

A necessary condition for maximal superintegrability in the relative motion is that the two distinct internal frequencies be rationally related [23, 32],

$$\frac{\Omega_N}{\Omega_F} = p \in \mathbb{Q},$$

equivalently,

$$\frac{2\kappa_1^{(4)}}{\kappa_1^{(4)} + \kappa_2^{(4)}} = p^2, \quad \kappa_2^{(4)} = \left(\frac{2}{p^2} - 1\right)\kappa_1^{(4)}.$$

Thus any rational ratio $1:p$ can be realized by a suitable choice of couplings. However, maximal superintegrability, and hence periodicity, does not by itself imply C_4 -equivariance.

For the explicit analytic four-body choreographies considered here, the relevant selection occurs in reduced one-sided or effectively single-sector families. Writing $\tau_4 := T/4$, the phase-matching conditions become

$$e^{i\Omega_F \tau_4} = e^{i\pi/2}, \quad e^{i\Omega_N \tau_4} = e^{i\pi} = -1.$$

If both sectors are active and $\Omega_N = p \Omega_F$ with $p \in \mathbb{Q}$, one may take $T = 2\pi/\Omega_F$, so that

$$\tau_4 = \frac{\pi}{2\Omega_F}.$$

The Nyquist condition then gives

$$e^{ip\pi/2} = -1, \quad p \equiv 2 \pmod{4}.$$

Hence the primitive reduced-family choreographic resonance is

$$\Omega_N = 2\Omega_F.$$

For the potential (9), this is equivalent to

$$\Omega_N = 2\omega\sqrt{\kappa_1^{(4)}}, \quad \Omega_F = \omega\sqrt{2(\kappa_1^{(4)} + \kappa_2^{(4)})}, \quad \kappa_2^{(4)} = -\frac{1}{2}\kappa_1^{(4)}.$$

4.3.1 Fragmentations

Only two synchronization patterns are compatible with the D_4 symmetry:

- (i) *Generic (2+2) decomposition (dimer splitting)*. The two diagonal modes oscillate independently. Particles (1, 3) and (2, 4) each form a synchronized dimer executing a two-body choreography, but the two dimers are dynamically independent (see Fig. 3). Accordingly, the residual time-shift symmetry is only C_2 .

- (ii) *Four-body choreography.* When specific initial conditions hold, the two diagonal modes phase-lock and combine into a single C_4 -equivariant motion. All four particles traverse the same closed curve with uniform quarterperiod time shifts (see Fig. 4). This is the unique four-body choreography compatible with D_4 symmetry.

A $(3+1)$ pattern does not arise in the present D_4 -resolved families and will not be considered further here.

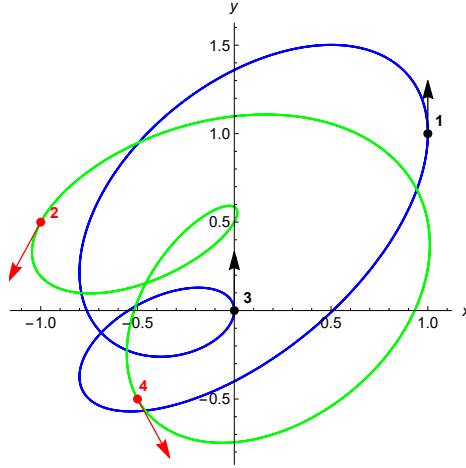


Fig. 3 Four-body D_4 -invariant quadratic system in the superintegrable $(1:2)$ regime ($\mu = 1$, $\omega = 1$, $\kappa_1^{(4)} = 1$, $\kappa_2^{(4)} = -\frac{1}{2}$) showing a $(2+2)$ choreographic fragmentation. Initial conditions at $t = 0$: $\mathbf{r}_1 = (1, 1)$, $\mathbf{r}_2 = (-1, \frac{1}{2})$, $\mathbf{r}_3 = (0, 0)$, $\mathbf{r}_4 = (-\frac{1}{2}, -\frac{1}{2})$; $\mathbf{p}_1 = (0, \frac{3}{2})$, $\mathbf{p}_2 = (-\frac{1}{2}, -1)$, $\mathbf{p}_3 = (0, \frac{1}{2})$, $\mathbf{p}_4 = (\frac{1}{2}, -1)$. Particles $(1, 3)$ and $(2, 4)$ form two synchronized dimers, each executing a two-body choreography with time shift $T/2$; the full motion is periodic but only C_2 -equivariant (hence not a single four-body choreography).

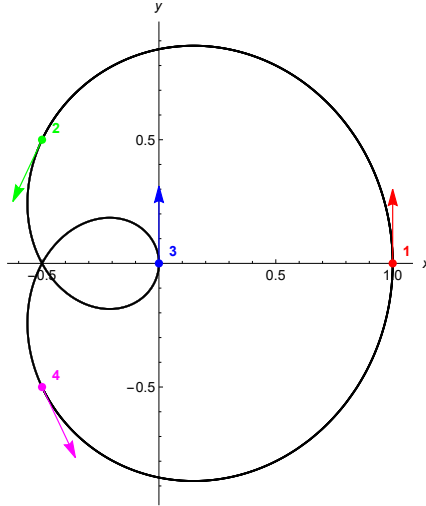


Fig. 4 Four-body (1:2) limaçon choreography in the superintegrable D_4 -invariant quadratic model with $\mu = 1$, $\omega = 1$, $\kappa_1^{(4)} = 1$, $\kappa_2^{(4)} = -\frac{1}{2}$ (hence $\Omega_F = 1$, $\Omega_N = 2$). Initial conditions at $t = 0$: $\mathbf{r}_1 = (1, 0)$, $\mathbf{r}_2 = (-\frac{1}{2}, \frac{1}{2})$, $\mathbf{r}_3 = (0, 0)$, $\mathbf{r}_4 = (-\frac{1}{2}, -\frac{1}{2})$; $\mathbf{p}_1 = (0, \frac{3}{2})$, $\mathbf{p}_2 = (-\frac{1}{2}, -1)$, $\mathbf{p}_3 = (0, \frac{1}{2})$, $\mathbf{p}_4 = (\frac{1}{2}, -1)$. All four particles traverse the same closed curve with time shift $T/4$, realizing the primitive 1:2 superintegrable four-body choreography.

4.4 Case $n = 5$

4.5 Hamiltonian and D_5 -invariant potential

For five equal masses in the plane, case $n = 5$, the most general quadratic D_5 -invariant Hamiltonian reads

$$\mathcal{H}_5 = \frac{1}{2\mu} \sum_{i=1}^5 \mathbf{p}_i^2 + V_5(r_{ij}), \quad i, j = 1, \dots, 5, \quad (11)$$

with 20-dimensional phase space. The potential $V_5(r_{ij})$ includes first- and second-neighbor couplings determined by the index structure of an abstract regular pentagon, see Fig. 5. Explicitly

$$V_5 = \frac{1}{2}\mu\omega^2 \left[\kappa_1^{(5)} (r_{12}^2 + r_{23}^2 + r_{34}^2 + r_{45}^2 + r_{15}^2) + \kappa_2^{(5)} (r_{13}^2 + r_{14}^2 + r_{24}^2 + r_{25}^2 + r_{35}^2) \right]. \quad (12)$$

A superintegrable choice is

$$\kappa_1^{(5)} = \frac{1}{2} \left(\frac{3}{\sqrt{5}} + 1 \right) > 0, \quad \kappa_2^{(5)} = -\frac{1}{2} \left(\frac{3}{\sqrt{5}} - 1 \right) < 0, \quad (13)$$

corresponding to a strong attractive coupling between nearest neighbors and a weaker repulsive coupling between second neighbors. Details of the separation of variables and the resulting trajectories are given in Appendix A.2.

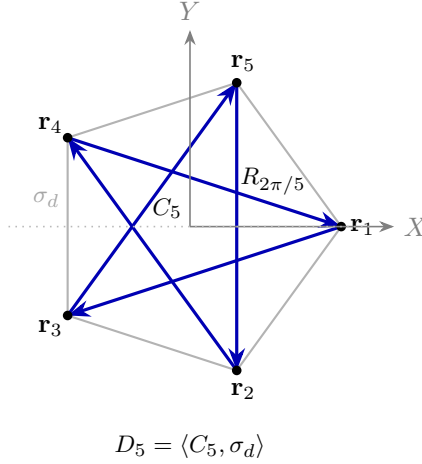


Fig. 5 Second-neighbor relative vectors for $n = 5$. Blue arrows represent the equivalent second-neighbor bonds. These variables diagonalize the quadratic D_5 -invariant Hamiltonian.

The pentagon in Fig. 5 is best understood by combining the spatiotemporal D_5 symmetry with the D_5 normal-mode (Fourier) decomposition of the center-of-mass dynamics. The dihedral action on the labels is generated by a cyclic relabeling r of order five and a reflection s , with $r^5 = s^2 = e$ and $sr s = r^{-1}$. In the present configuration-level formulation, C_5 -equivariance means cyclic relabeling of the particles combined with the time shift $T/5$, while full D_5 symmetry adds an appropriate reflection symmetry (typically up to relabeling and a time shift, and in reversible settings possibly time reversal). On the mode level, the internal space splits into two D_5 -invariant irreducible sectors, $H_{\text{int}} = H_1 \oplus H_2$ (doublets with characters $e^{2\pi i \ell / 5}$, $\ell = 1, 2$). If the motion lies in a single sector, the five trajectories are time-shifted copies of one curve and one obtains a genuine five-body single-trace choreography. By contrast, if both inequivalent sectors are excited, the motion may remain periodic when the corresponding frequencies are commensurate, but generic full-space multi-sector data do not satisfy the full C_5 phase-matching condition of Theorem 2. The generic outcome is therefore not a genuine five-body single-trace choreography, but a periodic multi-trace motion in which the bodies may organize into synchronized sub-choreographies (e.g. $(3 + 2)$ or $(2 + 2 + 1)$) rather than sharing a common geometric trace.

4.6 General frequencies, superintegrability, and choreographies

The general D_5 -invariant quadratic potential

$$V_5 = \frac{1}{2} \mu \omega^2 \left[\kappa_1^{(5)} \sum_{i=1}^5 r_{i,i+1}^2 + \kappa_2^{(5)} \sum_{i=1}^5 r_{i,i+2}^2 \right]$$

contains two independent couplings $\kappa_1^{(5)}$ and $\kappa_2^{(5)}$. Its quadratic form has one zero mode and four internal modes arranged in two doublets, with distinct frequencies

$$\Omega_1 = \omega \sqrt{\lambda_-}, \quad \Omega_2 = \omega \sqrt{\lambda_+},$$

where

$$\lambda_{\pm} = \frac{1}{2} \left[5(\kappa_1^{(5)} + \kappa_2^{(5)}) \pm \sqrt{5}(\kappa_1^{(5)} - \kappa_2^{(5)}) \right], \quad (14)$$

each with multiplicity 2, and reality requires $\lambda_{\pm} > 0$.

As in the case $n = 4$, the D_5 -invariant quadratic interaction produces only two distinct internal frequencies, each doubly degenerate. Thus full internal motions involve at most two frequency branches, so the issue is not a three-frequency obstruction of the type appearing at $n = 6$, but whether the active doublets can simultaneously satisfy the C_5 phase-matching condition.

Maximal superintegrability requires the two distinct frequencies to be commensurate,

$$\frac{\Omega_2}{\Omega_1} = p \in \mathbb{Q},$$

or equivalently,

$$\frac{\lambda_+}{\lambda_-} = p^2 = \frac{5(\kappa_1^{(5)} + \kappa_2^{(5)}) + \sqrt{5}(\kappa_1^{(5)} - \kappa_2^{(5)})}{5(\kappa_1^{(5)} + \kappa_2^{(5)}) - \sqrt{5}(\kappa_1^{(5)} - \kappa_2^{(5)})}.$$

Thus every rational p determines a one-parameter family of couplings for which the system is maximally superintegrable. However, maximal superintegrability, and hence periodicity, does not by itself imply five-body choreographic symmetry.

For the explicit analytic five-body choreographies considered here, the relevant selection again occurs in reduced one-sided families. If the two active doublets have frequencies Ω_1 and Ω_2 , their phases under the shift $T/5$ must satisfy

$$e^{i\Omega_1 T/5} = e^{2\pi i/5}, \quad e^{i\Omega_2 T/5} = e^{4\pi i/5}.$$

If $\Omega_2 = p \Omega_1$ with $p \in \mathbb{Q}$, comparison of the character phases gives

$$e^{i\Omega_2 T/5} = \left(e^{i\Omega_1 T/5} \right)^p,$$

which selects

$$p = 2.$$

Hence the primitive choreographic resonance in this explicit family is

$$\Omega_2 = 2\Omega_1,$$

the resonance that produces the fivefold limaçon-type choreography displayed below.

4.6.1 Fragmentations

Because the internal dynamics consists of two independent D_5 doublets, only a limited set of synchronization patterns can arise when global C_5 -equivariance fails:

(a) (3+2) fragmentation.

One doublet organizes a synchronized three-body sub-choreography, while the other organizes a synchronized dimer. The resulting motion has a residual C_3 time-shift symmetry on the three-body submotion, but it is not C_5 -equivariant and hence is not a five-body choreography. When the three-body and two-body submotions are supported on distinct closed curves, the overall motion is choreographically fragmented.

Remark. The C_3 appearing in (a) is not a geometric subgroup of the rotation group C_5 ; it is a dynamical cyclic symmetry acting on the three-body submotion. Concretely, it means that three particles traverse a common curve with time shifts of $T/3$, while the remaining two particles form an independent synchronized dimer. This illustrates that fragment symmetries need not coincide with subgroups of the ambient cyclic label symmetry.

(b) (2+2+1) fragmentation.

Each doublet produces a synchronized dimer on separate curves, while the remaining particle follows its own different trajectory (see Fig. 6). This configuration is equivariant under C_2 on each dimer but has no global C_5 time-shift symmetry.

(c) Full five-body choreography.

When the two doublets satisfy the (1:2) resonance $\Omega_2 = 2\Omega_1$ and the corresponding phase-matching condition, their superposition locks into the limaçon five-body choreography with full C_5 equivariance (see Fig. 7).

(d) Other patterns.

Beyond the (3+2) and (2+2+1) patterns discussed above, we do not pursue a further classification of possible fragmented motions in the present D_5 setting.

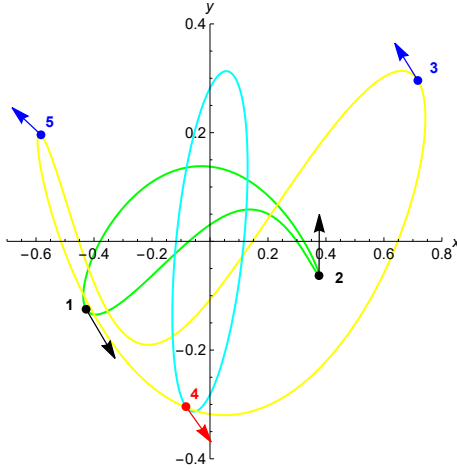


Fig. 6 Five-body D_5 -invariant quadratic system in the superintegrable (1 : 2) regime ($\mu = 1, \omega = 1, \kappa_1^{(5)} = \frac{1}{2}(\frac{3}{\sqrt{5}} + 1), \kappa_2^{(5)} = -\frac{1}{2}(\frac{3}{\sqrt{5}} - 1)$) showing a (2 + 2 + 1) fragmented periodic motion. Initial conditions at $t = 0$: $\mathbf{r}_1 = (-0.144427, 0.079180)$, $\mathbf{r}_2 = (0.659017, 0.140983)$, $\mathbf{r}_3 = (1.0, 0.5)$, $\mathbf{r}_4 = (0.2, -0.1)$, $\mathbf{r}_5 = (-0.3, 0.4)$; $\mathbf{p}_1 = (0.1, -0.090451)$, $\mathbf{p}_2 = (0.023607, -0.002254)$, $\mathbf{p}_3 = (-0.223607, 0.192705)$, $\mathbf{p}_4 = (0.2, -0.15)$, $\mathbf{p}_5 = (-0.1, 0.05)$. Two synchronized dimers and one isolated particle evolve on distinct closed curves; the full motion is periodic but not C_5 -equivariant. In the terminology adopted here, this is a choreographic fragmentation.

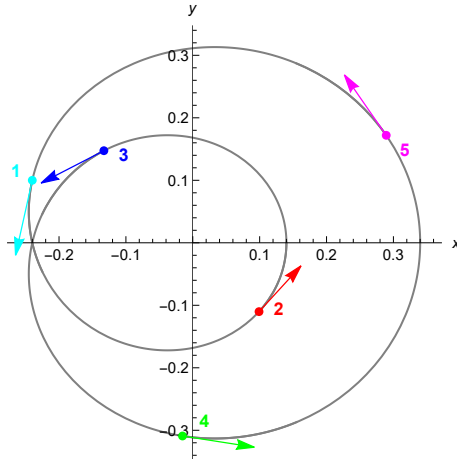


Fig. 7 Five-body C_5 -equivariant limaçon choreography in the superintegrable D_5 -invariant quadratic model with $\mu = 1, \omega = 1, \kappa_1^{(5)} = \frac{1}{2}(\frac{3}{\sqrt{5}} + 1), \kappa_2^{(5)} = -\frac{1}{2}(\frac{3}{\sqrt{5}} - 1)$, yielding the resonant spectrum $\Omega_2 = 2\Omega_1$. Initial conditions at $t = 0$, rotated by $\pi/2$ from the previous orientation, are $\mathbf{r}_1 = (-0.240000, 0.100000)$, $\mathbf{r}_2 = (0.099058, -0.110167)$, $\mathbf{r}_3 = (-0.132943, 0.147352)$, $\mathbf{r}_4 = (-0.015386, -0.309155)$, $\mathbf{r}_5 = (0.289270, 0.171970)$; $\mathbf{p}_1 = (-0.100000, -0.480000)$, $\mathbf{p}_2 = (0.251235, 0.293223)$, $\mathbf{p}_3 = (-0.375605, -0.207107)$, $\mathbf{p}_4 = (0.537409, -0.089550)$, $\mathbf{p}_5 = (-0.313039, 0.483434)$. All particles traverse the same closed curve with uniform time shift $T/5 = 2\pi/(5\Omega_1)$, realizing a noncircular pentagonal (limaçon-type) five-body choreography.

4.7 Structural lessons from low n

The cases $n = 4$ and $n = 5$ already exhibit the basic mechanism: periodicity alone is insufficient for choreography, while C_n -equivariance requires an additional compatibility between time evolution and symmetry. At the same time, these low- n systems remain comparatively rigid from the symmetry-resolved viewpoint, since only two inequivalent internal sectors are present. As a result, the relevant reduced families and invariant subspaces can be analyzed explicitly, and the contrast between single-trace and fragmented motion can be followed in closed form. In particular, the explicit four- and five-body choreographies arise when the active motion is effectively confined to a reduced or phase-locked family, whereas generic multi-sector excitations already produce fragmented periodic motion.

At $n = 6$, the symmetry-resolved sector structure becomes richer: three inequivalent internal sectors coexist and two independent resonance ratios appear. The six-body problem is therefore the first symmetry-richer case, and the natural setting in which to distinguish periodicity, full-space choreographies, reduced-subspace choreographies, and fragmented periodic motions with reduced symmetry.

5 Case $n = 6$: nondegenerate commensurability, exact degeneracy, and fragmentation

The six-body system is the first value of n for which three inequivalent internal symmetry sectors coexist: two doublets and one Nyquist singlet. In contrast to the lower cases $n = 4, 5$, two independent resonance ratios appear, so that even maximally resonant superintegrable periodic motion need not collapse into a single geometric trace. The new phenomenon at $n = 6$ is therefore not a failure of full C_6 -equivariance to imply choreography, but the proliferation of periodic resonant motions with reduced symmetry, together with the distinguished role of exact degeneracies that can restore an effective one-sector structure and thereby support a genuine six-body choreography.

For $n = 6$, the internal dynamics already exhibits symmetry-induced modal degeneracies: the branches $\ell = 1, 2$ are D_6 doublets, while $\ell = 3$ is the Nyquist singlet. Against this background, the resonance 1:2:3 is a case of nondegenerate commensurability among three distinct branches, whereas 1:2:2 introduces an additional exact spectral degeneracy, $\Omega_2 = \Omega_3$. Both may support genuine six-body choreographies, but through different mechanisms.

5.1 Hamiltonian and D_6 -invariant quadratic potential

For six equal masses, the most general D_6 -invariant quadratic Hamiltonian reads

$$\begin{aligned} \mathcal{H}_6 &= \frac{1}{2\mu} \sum_{i=1}^6 \mathbf{p}_i^2 + \frac{1}{2} \mu \omega^2 \kappa_1^{(6)} (r_{12}^2 + r_{23}^2 + r_{34}^2 + r_{45}^2 + r_{56}^2 + r_{16}^2) \\ &+ \frac{1}{2} \mu \omega^2 \kappa_2^{(6)} (r_{13}^2 + r_{24}^2 + r_{35}^2 + r_{46}^2 + r_{15}^2 + r_{26}^2) \\ &+ \frac{1}{2} \mu \omega^2 \kappa_3^{(6)} (r_{14}^2 + r_{25}^2 + r_{36}^2). \end{aligned} \quad (15)$$

The potential contains three coupling parameters $\kappa_1^{(6)}, \kappa_2^{(6)}, \kappa_3^{(6)}$. Here, indices are understood modulo 6 and $r_{ij} = |\mathbf{r}_i - \mathbf{r}_j|$. The three couplings $\kappa_{1,2,3}^{(6)}$ correspond to first neighbors, second neighbors, and opposite vertices of an abstract hexagon.

Remark 5 (Normalization for the $n = 6$ example) In Eq. (15), the opposite-vertex terms

$$r_{14}^2 + r_{25}^2 + r_{36}^2$$

are written in the single-count convention. Relative to the uniform even- n convention of Section 2, this amounts to a rescaling by a factor of 2 in the Nyquist coupling. All frequency formulas in the present section are to be interpreted with this normalization.

5.2 Normal-mode structure and (maximal) superintegrability

After removal of the center-of-mass motion, diagonalization by the discrete Fourier transform yields three distinct internal stiffness eigenvalues λ_ℓ and frequencies $\Omega_\ell = \omega\sqrt{\lambda_\ell}$, $\ell = 1, 2, 3$:

$$\lambda_1 = \kappa_1^{(6)} + 3\kappa_2^{(6)} + 2\kappa_3^{(6)}, \quad \lambda_2 = 3\kappa_1^{(6)} + 3\kappa_2^{(6)}, \quad \lambda_3 = 4\kappa_1^{(6)} + 2\kappa_3^{(6)}. \quad (16)$$

The sectors $(\ell, 6 - \ell)$ with $\ell = 1, 2$ form two inequivalent two-dimensional D_6 irreducible representations (cosine-sine doublets), while the Nyquist sector $\ell = 3$ is one-dimensional.

Thus the degeneracies associated with the $\ell = 1, 2$ branches are already imposed by the D_6 symmetry, whereas the possible coincidence $\Omega_2 = \Omega_3$ represents an additional exact spectral degeneracy beyond this symmetry-induced structure.

Because the internal motion separates into uncoupled oscillators, the system is integrable and becomes maximally superintegrable whenever the independent ratios

$$\frac{\Omega_2}{\Omega_1} = p_1 \in \mathbb{Q}, \quad \frac{\Omega_3}{\Omega_1} = p_2 \in \mathbb{Q} \quad (17)$$

are rational. Equivalently, $\lambda_2/\lambda_1 = p_1^2$ and $\lambda_3/\lambda_1 = p_2^2$, which imposes two homogeneous linear relations among the three couplings and leaves a one-parameter family of maximally superintegrable Hamiltonians for each rational pair (p_1, p_2) .

| Setting | Resonance pattern | Dynamical meaning |
|--------------------------------------|--|---|
| Nondegenerate three-branch resonance | $\Omega_1 : \Omega_2 : \Omega_3 = 1 : 2 : 3$ | Commensurate resonance among three distinct frequency branches. The D_6 -induced modal degeneracies remain unchanged, and the three active sectors stay dynamically distinct. When the sector-wise phase-matching condition holds, this yields a genuine six-body single-trace choreography. |
| Additional exact degeneracy | $\Omega_1 : \Omega_2 : \Omega_3 = 1 : 2 : 2$ | Further exact spectral coincidence $\Omega_2 = \Omega_3$, beyond the modal degeneracies already imposed by D_6 . The coincidence $\Omega_2 = \Omega_3$ allows an effective sectoral description only under additional phase-locking or invariant-subspace constraints. When the corresponding phase-matching condition holds, it provides a distinct mechanism for a genuine six-body single-trace choreography. |
| Reduced invariant subspace | $\Omega_1 : \Omega_2 = 1 : 2$ | Obtained by suppressing one sector through the initial data (for example, the Nyquist mode). This yields an analytic reduced-subspace six-body choreography, but not a full three-sector statement. |

Table 2 Three distinct resonance settings in the six-body problem. The ratio $\Omega_1 : \Omega_2 : \Omega_3 = 1 : 2 : 3$ represents nondegenerate commensurability among three distinct branches, whereas $\Omega_1 : \Omega_2 : \Omega_3 = 1 : 2 : 2$ represents an additional exact degeneracy, $\Omega_2 = \Omega_3$, on top of the modal degeneracies already induced by D_6 . Both can support genuine six-body choreographies when the phase-matching condition of Theorem 2 is satisfied. The ratio $\Omega_1 : \Omega_2 = 1 : 2$ arises only after restriction to a proper invariant subspace.

Key point. Superintegrability, and hence periodicity, does not by itself determine whether a six-body periodic orbit is a choreography; that requires the symmetry realization condition of Theorem 2, which in the present full-configuration setting yields a genuine single-trace choreography by Corollary 1. Table 2 therefore separates three distinct situations: the nondegenerate commensurate resonance $1 : 2 : 3$ among three distinct frequency branches; the further exactly degenerate resonance $1 : 2 : 2$, characterized by the additional coincidence $\Omega_2 = \Omega_3$ beyond the modal degeneracies imposed by D_6 and allowing an effective sectoral description only when the relevant phase-locking or invariant-subspace constraints are also imposed; and the ratio $1 : 2$, which arises only after restriction to a proper invariant subspace. The first two can support genuine six-body single-trace choreographies when the phase-matching condition holds.

5.3 C_6 phase matching in the nondegenerate $1 : 2 : 3$ resonance

Let T denote the global period. The generator of C_6 acts on the ℓ th Fourier sector by the character e^{iq_ℓ} with

$$q_\ell = \frac{2\pi\ell}{6} = \frac{\ell\pi}{3}.$$

By Theorem 2, C_6 -equivariance is a condition on the sector amplitudes, not on the frequencies alone. In the one-sided family considered in this subsection, that amplitude condition reduces to the frequency-phase relations

$$e^{i\Omega_\ell T/6} = e^{iq_\ell} = e^{i\ell\pi/3}, \quad \ell \text{ active.} \quad (18)$$

If all three sectors $\ell = 1, 2, 3$ are active and remain dynamically distinct, the smallest positive solution of Eq. (18) is

$$\Omega_1 : \Omega_2 : \Omega_3 = 1 : 2 : 3. \quad (19)$$

Thus the resonance 1:2:3 should be understood as the basic *nondegenerate* C_6 -equivariant resonance among three distinct frequency branches. When the corresponding sectorwise phase-matching condition holds, the resulting motion is C_6 -equivariant and hence, by Corollary 1, a genuine single-trace six-body choreography.

5.4 Generic obstruction near the nondegenerate 1:2:3 resonance

The resonance relation (19) identifies the basic nondegenerate commensurate pattern among the three distinct frequency branches $\Omega_1, \Omega_2, \Omega_3$. When the corresponding sectorwise phase-matching condition (18) is satisfied, the resulting motion is C_6 -equivariant and therefore, by Corollary 1, a genuine single-trace six-body choreography. The relevant point here is different: outside these special phase-matched configurations, generic full-space multi-sector periodic data near the 1:2:3 resonance fail the full phase-matching condition of Theorem 2. Consequently, although the motion remains periodic by commensurability, it is generically not C_6 -equivariant and instead organizes into multi-trace motion, often with reduced symmetry and, in structured cases, choreographic fragmentation.

5.5 The further exactly degenerate 1:2:2 resonance

A second, structurally distinct six-body resonance occurs when the internal spectrum acquires an additional exact degeneracy beyond the modal degeneracies already imposed by D_6 . This happens at

$$\Omega_1 : \Omega_2 : \Omega_3 = 1 : 2 : 2, \quad (20)$$

i.e. when $\Omega_2 = \Omega_3$. This exact coincidence does not by itself erase the different C_6 characters of the $\ell = 2$ and $\ell = 3$ sectors. Rather, it creates the possibility of an effective one-sector description only after the corresponding amplitudes satisfy the appropriate phase-locking or invariant-subspace constraints. When those additional constraints are met, the sectorwise phase-matching condition of Theorem 2 yields a genuine six-body single-trace choreography.

5.6 Reduced-subspace choreographies

The six-body system may also exhibit choreographies on proper invariant linear subspaces obtained by suppressing one symmetry sector through the initial data. For instance, setting the Nyquist amplitude to zero restricts the dynamics to the two D_6 doublets. Within this reduced invariant subspace, the general amplitude-level

condition of Theorem 2 simplifies to the two-frequency relations

$$e^{i\Omega_1 T/6} = e^{i\pi/3}, \quad e^{i\Omega_2 T/6} = e^{2i\pi/3},$$

which select

$$\Omega_2 = 2\Omega_1.$$

This yields an analytic (1:2) six-body choreography on a proper invariant subspace. It is therefore distinct from both the nondegenerate full-space resonance 1:2:3 and the additionally degenerate full-space resonance 1:2:2: the mechanism here is sector suppression, not three-branch commensurability or extra spectral coincidence.

5.7 Concrete 1:2:3 example and fragmentation

A representative fully resonant choice is

$$(\kappa_1^{(6)}, \kappa_2^{(6)}, \kappa_3^{(6)}) = \left(2, -\frac{2}{3}, \frac{1}{2}\right),$$

for which (16) yields $\lambda_1 = 1$, $\lambda_2 = 4$, $\lambda_3 = 9$, hence

$$\Omega_1 : \Omega_2 : \Omega_3 = 1 : 2 : 3.$$

This realizes the basic nondegenerate commensurate resonance among the three distinct frequency branches. When the sectorwise phase-matching condition of Theorem 2 is satisfied, the resulting motion is C_6 -equivariant and therefore, by Corollary 1, a genuine single-trace six-body choreography. For generic initial data, however, commensurability alone does not enforce the required phase matching across all active sectors: the motion remains periodic, but typically becomes multi-trace and may have only reduced cyclic symmetry. In structured cases, it organizes into synchronized sub-choreographies supported on distinct curves, giving rise to choreographic fragmentation. Thus, in the present full-configuration formulation, the 1:2:3 resonance should be understood as a nondegenerate commensurate organizing pattern that supports both special phase-matched six-body choreographies and generic fragmented periodic motions.

5.7.1 Fragmented resonant motions

Not every rational resonance produces a six-body choreography in the geometric sense. Besides the choreographic cases, resonant excitations generically destroy the global $T/6$ time-shift relation. The nondegenerate resonance 1:2:3 yields periodic motion among three distinct frequency branches, but a genuine six-body choreography occurs only on the special phase-matched locus of Theorem 2. Away from that locus, generic resonant initial data produce periodic multi-trace motions with reduced cyclic symmetry. In structured cases the motion organizes into synchronized sub-choreographies supported on distinct curves, giving rise to choreographic fragmentation. In the present full-configuration formulation, any genuinely C_6 -equivariant

full-space motion is already a single-trace choreography by Corollary 1; accordingly, the $1 : 2 : 3$ resonance should be understood here as a nondegenerate three-branch commensurate resonance, not as a source of full-space equivariant fragmentation.

(a) (3+3) fragmentation (C_3 , time shift $T/3$).

If the two D_6 doublets satisfy the resonance $\Omega_2 = 2\Omega_1$ while the Nyquist mode is inactive or does not phase-lock to them, the motion is typically C_3 -equivariant rather than C_6 -equivariant. The particles split into two synchronized triples,

$$\{1, 3, 5\}, \quad \{2, 4, 6\},$$

each executing a three-body sub-choreography with time shift $T/3$. The two triples are dynamically independent; in our sense this constitutes *fragmentation* precisely when the two triples are supported on distinct closed curves (up to rigid motions).

(b) (2+2+2) fragmentation (C_2 , time shift $T/2$).

If the Nyquist mode resonates with the $\ell = 1$ doublet while the $\ell = 2$ doublet is inactive (or nonresonant), the system splits into three synchronized dimers,

$$(1, 4), \quad (2, 5), \quad (3, 6),$$

each invariant under a half-period time shift $T/2$. The three dimers are dynamically independent; in our view, this constitutes *fragmentation* precisely when the dimers trace distinct closed curves (up to rigid motions), see Fig. 8.

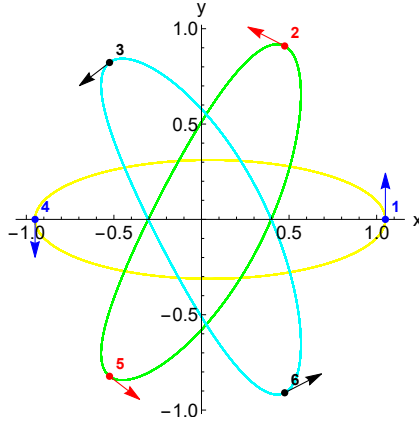


Fig. 8 Six-body motion showing a $(2 + 2 + 2)$ choreographic fragmentation. We used $(\kappa_1^{(6)}, \kappa_2^{(6)}, \kappa_3^{(6)}) = (2, -\frac{2}{3}, \frac{1}{2})$ and $\mu = \omega = 1$. Initial conditions at $t = 0$: $\mathbf{r}_1 = (1.05, 0)$, $\mathbf{r}_2 = (0.475, 0.909327)$, $\mathbf{r}_3 = (-0.525, 0.822724)$, $\mathbf{r}_4 = (-0.95, 0)$, $\mathbf{r}_5 = (-0.525, -0.822724)$, $\mathbf{r}_6 = (0.475, -0.909327)$; $\mathbf{p}_1 = (0, 0.341)$, $\mathbf{p}_2 = (-0.295315, 0.139500)$, $\mathbf{p}_3 = (-0.241621, -0.170500)$, $\mathbf{p}_4 = (0, -0.279000)$, $\mathbf{p}_5 = (0.241621, -0.170500)$, $\mathbf{p}_6 = (0.295315, 0.139500)$. The six particles split into three synchronized dimers, each dimer executing a two-body choreography (a $(2 + 2 + 2)$ fragmentation of the full six-body motion).

(c) *Full six-body choreography (C_6 , time shift $T/6$).*

When the double resonance

$$\Omega_2 = \Omega_3 = 2\Omega_1$$

holds together with the corresponding phase-matching condition, the active internal modes transform compatibly under C_6 and lock into a fully C_6 -equivariant motion. All six particles traverse the same closed curve with uniform time shifts of $T/6$, i.e.

$$\mathbf{r}_{i+1}(t) = \mathbf{r}_i\left(t + \frac{T}{6}\right).$$

Other rational resonances may still yield periodic, maximally superintegrable motions, but they fail to realize the global $T/6$ time-shift relation in the full phase space and instead exhibit reduced time-shift symmetry and/or fragmentation.

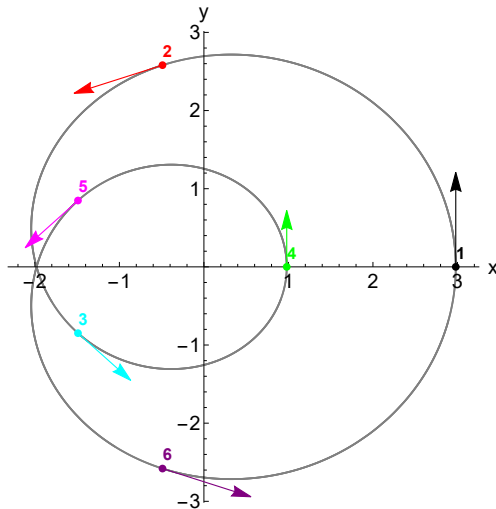


Fig. 9 Six-body choreography in the planar quadratic model. We used $(\kappa_1^{(6)}, \kappa_2^{(6)}, \kappa_3^{(6)}) = (\frac{7}{2}, \frac{1}{2}, -1)$ and $\mu = \omega = 1$. Initial conditions at $t = 0$: $\mathbf{r}_1 = (2.98, 0)$, $\mathbf{r}_2 = (-0.49, 2.580756)$, $\mathbf{r}_3 = (-1.49, -0.848705)$, $\mathbf{r}_4 = (0.98, 0)$, $\mathbf{r}_5 = (-1.49, 0.848705)$, $\mathbf{r}_6 = (-0.49, -2.580756)$; $\mathbf{p}_1 = (0, 4.96)$, $\mathbf{p}_2 = (-4.295486, -1.48)$, $\mathbf{p}_3 = (2.563435, -2.48)$, $\mathbf{p}_4 = (0, 2.96)$, $\mathbf{p}_5 = (-2.563435, -2.48)$, $\mathbf{p}_6 = (4.295486, -1.48)$. All six particles move on the same curve determined by these initial data, forming a six-body choreographic motion. This choice realizes the degenerate locking $\Omega_2 = \Omega_3 = 2\Omega_1$ (the 1:2:2 resonance).

(d) *Other fragmentations.*

Beyond the (3+3) and (2+2+2) patterns discussed above, we do not pursue a further classification of possible fragmented motions in the present D_6 setting.

5.7.2 Summary for $n = 6$

For $n = 6$, one must distinguish three different resonance settings. The ratio 1:2:3 is the basic nondegenerate commensurate resonance among three distinct branches; the

ratio 1:2:2 is distinguished by the additional exact degeneracy $\Omega_2 = \Omega_3$; and the ratio 1:2 arises only on a proper invariant subspace. The first two can both support genuine six-body choreographies when the full phase-matching condition holds, but through different mechanisms: the former through nondegenerate commensurability, the latter through additional exact degeneracy. Generic nearby commensurate motions that fail phase matching remain periodic but multi-trace, often with reduced symmetry and, in structured cases, choreographic fragmentation.

6 Periodic multi-trace motion and choreographic fragmentation

From $n = 6$ onward, the internal decomposition involves enough inequivalent sectors that resonant periodic motions become genuinely nonrigid. The key point, however, is that in the present full-configuration formulation

$$C_n\text{-equivariance} \implies \text{single-trace choreography}$$

by Corollary 1. The relevant obstruction is therefore not a failure of full equivariance to imply choreography, but rather the generic failure of full equivariance itself in nondegenerate multi-sector periodic families.

Within this broader setting, fragmented periodic splittings already occur in the low- n examples of Sections 4 and 5, while $n = 6$ is the first case in which several inequivalent sectors can interact through two independent resonance ratios. This yields a richer hierarchy of periodic motions, including full-space choreographies, reduced subspace choreographies, and structured fragmented motions with only reduced cyclic symmetry.

6.1 Hierarchy of notions

Let $\mathbf{R}(t)$ be a T -periodic collision-free solution of a quadratic D_n -invariant system. We distinguish:

- **Periodicity:** $\mathbf{R}(t + T) = \mathbf{R}(t)$.
- **Full C_n -equivariance:** periodic motion satisfying the full amplitude-level condition of Theorem 2, namely Eq. (7), in every active sector.
- **Single-trace choreography:** all particles traverse one geometric curve with uniform delay T/n .
- **Choreographic fragmentation:** a T -periodic multi-trace motion in which the particle trajectories split into $k > 1$ synchronized sub-choreographies supported on distinct closed curves.

In the present framework, the second notion implies the third: full C_n -equivariance of the configuration already yields a single-trace choreography. Fragmentation therefore belongs naturally to the class of periodic motions that fail full equivariance, or to reduced-symmetry / reduced-subspace constructions, see Tables 3 and 4.

| Notion | Defining property | Geometric outcome |
|-----------------------------|--|---|
| Periodicity | The active frequencies are commensurate | Closed motion |
| Full C_n -equivariance | Eq. (7) holds in every active sector | Correct global space-time symmetry under cyclic relabeling and time shift |
| Single-trace choreography | Configuration-level C_n -equivariance of the full motion (equivalently, the uniform-delay relation of Corollary 1) | One common trace |
| Choreographic fragmentation | Periodic multi-trace motion organized into synchronized sub-choreographies, typically without full C_n -equivariance | Several synchronized traces |

Table 3 Hierarchy of notions used in the paper.

| n | Couplings | Freq. branches | Distinguished behaviours |
|-----|-----------|----------------|---|
| 4 | 2 | 2 | Special phase-matched 1 : 2 four-body choreography; fragmented (2 + 2) motions |
| 5 | 2 | 2 | Special phase-matched 1 : 2 five-body choreography; fragmented (3 + 2) and (2 + 2 + 1) motions |
| 6 | 3 | 3 | Phase-matched 1 : 2 : 3 six-body choreography; additionally degenerate 1 : 2 : 2 six-body choreography; reduced-subspace 1 : 2 choreography; fragmented (3 + 3) and (2 + 2 + 2) motions |

Table 4 Summary of the low- n cases analyzed explicitly.

Remark 6 (Terminology) Throughout the paper, “fragmentation” refers to a structured multi-trace periodic motion splitting into synchronized sub-choreographies on distinct traces. Hence, this notion is not full C_n -equivariant. In the present formulation, if the full equivariance condition of Theorem 2 does hold for the entire configuration, then Corollary 1 yields a single-trace choreography rather than a fragmented motion.

6.2 Mechanism

The internal dynamics decomposes as

$$H_{\text{int}} = \bigoplus_{\ell=1}^{\lfloor n/2 \rfloor} H_{\ell},$$

where each H_{ℓ} carries a fixed C_n character. The phase-matching condition of Theorem 2 enforces compatibility between time evolution and cyclic relabeling sector by sector. When it holds in every active sector, the resulting full configuration is C_n -equivariant and therefore, by Corollary 1, a single-trace choreography.

The geometric richness appears when several inequivalent sectors are simultaneously active but the full phase-matching condition fails, or when one works in reduced one-sided families or proper invariant subspaces. In such cases the motion may remain periodic and organize into synchronized sub-choreographies on distinct traces, giving rise to choreographic fragmentation.

6.3 Large- n structure: sector proliferation, phase matching, and multi-trace motion

For $n > 6$, the same symmetry-resolved framework applies, but the larger number of inequivalent Fourier sectors leaves room for increasingly intricate resonance and phase-matching structures. In the center-of-mass frame, the internal space decomposes as $\mathcal{H}_{\text{int}} = \bigoplus_{\ell=1}^{\lfloor n/2 \rfloor} \mathcal{H}_\ell$, where each \mathcal{H}_ℓ is a D_n -invariant isotypic component carrying a fixed C_n character. As n grows, generic initial data may activate several inequivalent sectors. Consequently, even when the active frequencies are commensurate and the motion is periodic, full C_n -equivariance requires the amplitude-level phase-matching condition of Theorem 2 to hold simultaneously across the full active set.

The large- n decision structure is therefore the same as in the low-dimensional examples. First, the motion is periodic only when the active frequencies are rationally commensurate, so that all excited sectors close after a common time T . Second, if the motion is periodic, it is fully C_n -equivariant only if the sectorwise phase-matching condition holds in every active sector. In reduced one-sided families or effectively single-sector settings created by exact degeneracy, this condition may simplify to the frequency-phase relations seen in the low- n cases. Third, whenever full C_n -equivariance holds for the full configuration, Corollary 1 yields a genuine single-trace n -body choreography. By contrast, when commensurability holds but full phase matching fails, the motion remains periodic but is generically multi-trace; in structured cases, the active sectors organize into synchronized sub-choreographies on distinct curves, producing choreographic fragmentation.

Thus, for $n > 6$, the simultaneous satisfaction of the full phase-matching conditions becomes progressively more restrictive, while commensurate periodic motions with reduced symmetry and multi-trace structure should become increasingly prevalent. Within the present quadratic D_n -invariant framework, genuine full-space choreographies arise only on special phase-matched loci or in regimes where exact degeneracies reorganize the active motion into an effective one-sector structure. Accordingly, the fragmented scenarios exhibited explicitly for $n = 4, 5, 6$ should be viewed as the first concrete manifestations of a broader large- n pattern of commensurate but non-phase-matched multi-sector dynamics, rather than as an exhaustive classification for all $n \geq 6$.

7 Conclusions and outlook

We have analyzed choreographic motion in quadratic D_n -invariant n -body systems from a unified symmetry-theoretic perspective. The central message of this work is that *algebraic resonance and superintegrability are not sufficient to produce choreographies*. Instead, the existence of a single-trace n -body choreography is governed by a representation-theoretic phase-matching condition and, depending on the dynamical setting, by whether the active symmetry sectors either satisfy that condition simultaneously or reorganize through exact degeneracy into an effective one-sector structure.

Our main results can be summarized as follows.

First, we formulated a general C_n -equivariance (phase-matching) criterion for quadratic D_n -invariant systems. In the present full-configuration formulation, within the collision-free sector, this criterion yields the choreography relation directly: once the configuration-level C_n symmetry is realized, the motion is already a genuine simple (single-trace) choreography.

Second, we showed that superintegrability and commensurability control periodicity but do not by themselves produce choreographies. The decisive additional ingredient is the phase-matching condition of Theorem 2.

Third, we identified $n = 6$ as the first symmetry-richer case, because three inequivalent internal sectors coexist and two independent resonance ratios appear. This forces a distinction between full-space choreographies, reduced-subspace choreographies, and fragmented periodic motions with reduced symmetry.

Fourth, we clarified the structural difference between the two principal six-body resonances. The ratio 1:2:3 is a case of nondegenerate commensurability among three distinct frequency branches, whereas the ratio 1:2:2 is distinguished by the additional exact degeneracy $\Omega_2 = \Omega_3$, beyond the modal degeneracies already imposed by D_6 . Both can support genuine six-body choreographies when the phase-matching condition holds, but through different mechanisms: the former through nondegenerate commensurability, the latter through additional exact degeneracy.

Finally, we introduced the notion of choreographic fragmentation as a natural language for structured multi-trace periodic motion organized into synchronized sub-choreographies on distinct traces. In the low- n examples this already appears through fragmented periodic splittings with reduced cyclic symmetry, and for larger n it provides a useful description of resonant multi-sector motions that fail the full equivariance condition of Theorem 2.

Taken together, these results clarify the role of symmetry in choreographic dynamics within the quadratic D_n -invariant setting studied here. In this class of models, choreographies should not be viewed as the generic expression of superintegrability, but rather as special configurations in which resonance, symmetry, and, in distinguished cases, exact degeneracy align to produce a single geometric trace.

Several directions for future work suggest themselves. It would be natural to investigate the persistence of choreographic and fragmented motions under nonlinear perturbations of the quadratic Hamiltonian, as well as their stability properties. More generally, the representation-theoretic mechanism identified here may provide a useful organizing principle for choreographies in broader classes of many-body systems, including non-Hamiltonian or driven settings.

We hope that the distinction between equivariance, choreography, and fragmentation emphasized in this work will help clarify the structure of collective motion in symmetric dynamical systems.

Declaration of competing interest

The authors declare that they have no known competing financial interests or personal relationships that could have appeared to influence the work reported in this paper.

Data availability

No data was used for the research described in the article.

References

- [1] Moore, C.: Braids in classical dynamics. *Physical Review Letters* **70**(24), 3675–3679 (1993) <https://doi.org/10.1103/PhysRevLett.70.3675>
- [2] Chenciner, A., Montgomery, R.: A remarkable periodic solution of the three-body problem in the case of equal masses. *Annals of Mathematics* **152**(3), 881–901 (2000) <https://doi.org/10.2307/2661357>
- [3] Simó, C.: Dynamical properties of the figure-eight solution of the three-body problem. In: Celletti, A., Simó, C. (eds.) *Celestial Mechanics. Contemporary Mathematics*, vol. 292, pp. 209–228. American Mathematical Society, Providence, RI (2002)
- [4] Marchal, C.: *The Three-Body Problem*. Elsevier, Amsterdam (2012)
- [5] Marchal, C.: How the method of minimization of action avoids singularities. *Celestial Mechanics and Dynamical Astronomy* **83**(1–4), 325–353 (2002) <https://doi.org/10.1023/A:1020128408706>
- [6] Barutello, V., Terracini, S.: Action minimizing orbits in the n -body problem with simple choreography constraint. *Nonlinearity* **17**(6), 2015–2039 (2004) <https://doi.org/10.1088/0951-7715/17/6/002>
- [7] Ferrario, D., Terracini, S.: On the existence of collisionless equivariant minimizers for the classical n -body problem. *Inventiones Mathematicae* **155**(2), 305–362 (2004) <https://doi.org/10.1007/s00222-003-0322-7>
- [8] Barutello, V., Ferrario, D., Terracini, S.: Symmetry groups of the planar n -body problem and action-minimizing solutions. *Archive for Rational Mechanics and Analysis* **190**(1), 189–237 (2008) <https://doi.org/10.1007/s00205-008-0131-7>
- [9] Chenciner, A., Féjóz, J., Montgomery, R.: Rotating eights: I. the three γ_i families. *Nonlinearity* **18**(3), 1407–1424 (2005) <https://doi.org/10.1088/0951-7715/18/3/024>
- [10] Simó, C.: New families of solutions in the n -body problem. In: Casacuberta, C., Miró-Roig, R.M., Verdera, J. (eds.) *European Congress of Mathematics. Progress in Mathematics*, vol. 201, pp. 101–115. Birkhäuser, Basel (2001)
- [11] Chenciner, A., Gerver, J., Montgomery, R., Simó, C.: Simple choreographic motions of N bodies: A preliminary study. In: Newton, P., Holmes, P., Weinstein, A. (eds.) *Geometry, Mechanics, and Dynamics*, pp. 287–308. Springer, New York,

- NY (2002). https://doi.org/10.1007/0-387-21791-6_9
- [12] Yu, G.: Simple choreographies of the planar newtonian N -body problem. *Archive for Rational Mechanics and Analysis* **225**, 901–935 (2017) <https://doi.org/10.1007/s00205-017-1116-1>
- [13] Barutello, V., Terracini, S.: Double choreographical solutions for n -body type problems. *Celestial Mechanics and Dynamical Astronomy* **95**(1–4), 67–80 (2006) <https://doi.org/10.1007/s10569-006-9030-0>
- [14] Montgomery, R.: The n -body problem, the braid group, and action-minimizing periodic solutions. *Nonlinearity* **11**(2), 363–376 (1998) <https://doi.org/10.1088/0951-7715/11/2/011>
- [15] Boyland, P.: Topological methods in surface dynamics. *Topology and its Applications* **58**(3), 223–298 (1994) [https://doi.org/10.1016/0166-8641\(94\)00147-2](https://doi.org/10.1016/0166-8641(94)00147-2)
- [16] Kapela, T., Simó, C.: Computer assisted proofs for nonsymmetric planar choreographies and for stability of the eight. *Nonlinearity* **20**(5), 1241 (2007) <https://doi.org/10.1088/0951-7715/20/5/010>
- [17] Fujiwara, T., Fukuda, H., Ozaki, H.: Choreographic three bodies on the lemniscate. *Journal of Physics A: Mathematical and General* **36**(11), 2791 (2003) <https://doi.org/10.1088/0305-4470/36/11/310>
- [18] Pérez-Chavela, E., Santoprete, M.: Convex four-body central configurations with some equal masses. *Archive for Rational Mechanics and Analysis* **185**, 481–494 (2007) <https://doi.org/10.1007/s00205-006-0047-z>
- [19] Diacu, F., Pérez-Chavela, E., Santoprete, M.: The n -body problem in spaces of constant curvature. part I: Relative equilibria. *Journal of Nonlinear Science* **22**, 247–266 (2012) <https://doi.org/10.1007/s00332-011-9116-z>
- [20] Miller, W., Post, S., Winternitz, P.: Classical and quantum superintegrability with applications. *Journal of Physics A: Mathematical and Theoretical* **46**, 423001 (2013) <https://doi.org/10.1088/1751-8113/46/42/423001>
- [21] Tempesta, P., Winternitz, P., Harnad, J., Miller Jr., W., Pogosyan, G., Rodríguez, M.A. (eds.): *Superintegrability in Classical and Quantum Systems*. CRM Proceedings & Lecture Notes, vol. 37. American Mathematical Society, Providence, RI (2004)
- [22] Calogero, F.: Solution of the one-dimensional n -body problem with quadratic and/or inversely quadratic pair potentials. *Journal of Mathematical Physics* **12**(3), 419–436 (1971) <https://doi.org/10.1063/1.1665604>
- [23] Perelomov, A.M.: *Integrable Systems of Classical Mechanics and Lie Algebras*.

Birkhäuser, Basel (1990)

- [24] Escobar-Ruiz, A.M., Fernández-Guasti, M.: On the four-body limaçon choreography: maximal superintegrability and choreographic fragmentation. *Celestial Mechanics and Dynamical Astronomy* **137**(24) (2025) <https://doi.org/10.1007/s10569-025-10255-1>
- [25] Escobar-Ruiz, A.M., Azuaje, R.: On particular integrability in classical mechanics. *Journal of Physics A: Mathematical and Theoretical* **57**(10), 105202 (2024) <https://doi.org/10.1088/1751-8121/ad2a1c>
- [26] Turbiner, A.V.: Particular integrability and (quasi)-exact-solvability. *Journal of Physics A: Mathematical and Theoretical* **46**(2), 025203 (2012) <https://doi.org/10.1088/1751-8113/46/2/025203>
- [27] Hamermesh, M.: *Group Theory and Its Application to Physical Problems*. Addison-Wesley, Reading, MA (1962)
- [28] Tinkham, M.: *Group Theory and Quantum Mechanics*. Dover Publications, New York (2003). Reprint of the 1964 McGraw–Hill edition
- [29] Fulton, W., Harris, J.: *Representation Theory: A First Course*. Graduate Texts in Mathematics, vol. 129. Springer, New York (1991)
- [30] Fernández-Guasti, M.: Analytic four-body limaçon choreography. *Celestial Mechanics and Dynamical Astronomy* **137**(4) (2025) <https://doi.org/10.1007/s10569-024-10235-x>
- [31] Fernandez-Guasti, M., Fujiwara, T., Pérez-Chavela, E., Zhu, S.: N-body choreographies on a p-limaçon curve. *Journal of Differential Equations* **454**, 113940 (2026) <https://doi.org/10.1016/j.jde.2025.113940>
- [32] Evans, N.W.: Superintegrability in classical mechanics. *Physical Review A* **41**(10), 5666–5676 (1990) <https://doi.org/10.1103/PhysRevA.41.5666>

A Separation of variables: normal mode decomposition

This appendix collects technical details underlying the explicit solutions discussed in the main text. For completeness, we present the separation of variables, normal-mode coordinates, and representative trajectory formulas for $n = 4, 5, 6$, as well as for general n .

We work in the center-of-mass frame and exploit the block-circulant structure of the quadratic D_n -invariant interaction matrix. Diagonalization by the discrete Fourier transform reduces the relative dynamics to a collection of uncoupled planar harmonic oscillators, each associated with an irreducible representation of D_n .

Throughout this Appendix we use real symmetry-adapted normal coordinates (for example $s_i, u_{c\ell}, u_{s\ell}$) rather than the complex Fourier coefficients U_ℓ used in the main text. These are equivalent descriptions: the appendix coordinates are the real cosine-sine decomposition of the sectors introduced in Theorem 2. The correspondence with the complex Fourier-sector notation of Section 2 is summarized in the remark following Theorem 2; throughout this appendix we use the equivalent real symmetry-adapted coordinates.

A.1 Case $n = 4$

In the original vectorial coordinates $\mathbf{r}_i \in \mathbb{R}^2$, the potential (9) with coupling constants (10) is not diagonal. However, because it is quadratic, one may perform the linear point transformation

$$\begin{pmatrix} \mathbf{s}_0 \\ \mathbf{s}_1 \\ \mathbf{s}_2 \\ \mathbf{s}_3 \end{pmatrix} = M \begin{pmatrix} \mathbf{r}_1 \\ \mathbf{r}_2 \\ \mathbf{r}_3 \\ \mathbf{r}_4 \end{pmatrix}, \quad \theta_4 = \frac{\pi}{2},$$

where $M = M(\theta_4)$ is the orthogonal 8×8 matrix¹

$$M = \begin{pmatrix} \frac{1}{2} & \frac{1}{2} & \frac{1}{2} & \frac{1}{2} \\ 0 & -\frac{1}{\sqrt{2}} & 0 & \frac{1}{\sqrt{2}} \\ \frac{1}{\sqrt{2}} & 0 & -\frac{1}{\sqrt{2}} & 0 \\ -\frac{1}{\sqrt{2}} & \frac{1}{\sqrt{2}} & -\frac{1}{\sqrt{2}} & \frac{1}{\sqrt{2}} \end{pmatrix}.$$

In terms of the vector coordinates $\mathbf{s}_i \in \mathbb{R}^2$, this transformation diagonalizes the Hamiltonian (8):

$$\mathcal{H}_4 = \frac{1}{2\mu} (\mathbf{P}_0^2 + \mathbf{P}_1^2 + \mathbf{P}_2^2 + \mathbf{P}_3^2) + \frac{1}{2}\mu\omega^2 (s_1^2 + s_2^2 + 4s_3^2),$$

where \mathbf{s}_0 describes the center of mass and $s_i = |\mathbf{s}_i|$. Therefore, the internal dynamics (relative motion) decomposes into three harmonic modes: a doubly degenerate pair with frequency $\Omega_1 = \Omega_2 = \omega$ and a Nyquist mode with frequency $\Omega_3 = 2\omega$. The **Nyquist mode** is the highest discrete internal frequency, corresponding to the Fourier index $k = n/2$ for even n , in which adjacent particles oscillate exactly out of phase ($e^{i\pi} = -1$). The frequency of the mode associated with the center-of-mass motion vanishes identically.

Normalization remark. For even n , the general D_n potential (see section 2.2)

$$V_n = \frac{1}{2}\mu\omega^2 \sum_{k=1}^{\lfloor n/2 \rfloor} \kappa_k^{(n)} \sum_{i=1}^n (\mathbf{r}_i - \mathbf{r}_{i+k})^2,$$

¹Each entry in M is a 2×2 diagonal matrix.

counts opposite-vertex bonds ($k = n/2$) twice. For $n = 4$ we list these bonds only once; therefore

$$\kappa_2^{(4)} \mapsto 2\kappa_2^{(4)}$$

when comparing with the general formulas. With this convention, the spectra for $n = 4$ agree with the uniform n -body expressions.

A.1.1 Trajectories in the center-of-mass frame

For the Hamiltonian (8) with coupling constants (10), the explicit solutions of Hamilton's equations of motion, expressed in Cartesian coordinates, are

$$\begin{aligned} \mathbf{r}_1(t) &= \frac{1}{2} [\mathbf{r}_{13}(0) \cos(\omega t) + \mathbf{r}_{13}^+(0) \cos(2\omega t)] + \frac{1}{4\mu\omega} [2\mathbf{p}_{13}(0) \sin(\omega t) + \mathbf{p}_{13}^+(0) \sin(2\omega t)], \\ \mathbf{r}_2(t) &= \frac{1}{2} [\mathbf{r}_{24}(0) \cos(\omega t) + \mathbf{r}_{24}^+(0) \cos(2\omega t)] + \frac{1}{4\mu\omega} [2\mathbf{p}_{24}(0) \sin(\omega t) + \mathbf{p}_{24}^+(0) \sin(2\omega t)], \\ \mathbf{r}_3(t) &= \mathbf{r}_1(t \pm 2\tau), \quad \mathbf{r}_4(t) = \mathbf{r}_2(t \pm 2\tau), \end{aligned} \tag{21}$$

with $\tau = \pi/(2\omega)$ and where

$$\mathbf{r}_{ij}^+ = \mathbf{r}_i + \mathbf{r}_j, \quad \mathbf{p}_{ij}^+ = \mathbf{p}_i + \mathbf{p}_j.$$

In the center-of-mass frame, $\mathbf{r}_{13}^+(t) = -\mathbf{r}_{24}^+(t)$ and $\mathbf{p}_{13}^+(t) = -\mathbf{p}_{24}^+(t)$. In (21), it is evident that only two frequencies are present: ω and 2ω . This is a consequence of the exact separation of variables into two uncoupled commensurable harmonic oscillators. Hence, it corresponds to a maximally superintegrable system [24]. In general, (21) describes two independent 2-body choreographies. Under special initial data, these two synchronized two-body sub-choreographies merge into a single four-body choreography.

A.2 Case $n = 5$

Introduce the real discrete Fourier coordinates

$$\begin{pmatrix} \mathbf{u}_0 \\ \mathbf{u}_1 \\ \mathbf{u}_2 \\ \mathbf{u}_3 \\ \mathbf{u}_4 \end{pmatrix} = W \begin{pmatrix} \mathbf{r}_1 \\ \mathbf{r}_2 \\ \mathbf{r}_3 \\ \mathbf{r}_4 \\ \mathbf{r}_5 \end{pmatrix}, \quad \theta_5 = \frac{2\pi}{5},$$

where W is the orthonormal 10×10 matrix

$$W = \begin{pmatrix} \frac{1}{\sqrt{5}} & \frac{1}{\sqrt{5}} & \frac{1}{\sqrt{5}} & \frac{1}{\sqrt{5}} & \frac{1}{\sqrt{5}} \\ \sqrt{\frac{2}{5}} & \sqrt{\frac{2}{5}}c_1^- & -\sqrt{\frac{2}{5}}c_1^+ & -\sqrt{\frac{2}{5}}c_1^+ & \sqrt{\frac{2}{5}}c_1^- \\ 0 & \frac{\sqrt{c_1^+}}{5^{1/4}} & \frac{\sqrt{c_1^-}}{5^{1/4}} & -\frac{\sqrt{c_1^-}}{5^{1/4}} & -\frac{\sqrt{c_1^+}}{5^{1/4}} \\ \sqrt{\frac{2}{5}} & -\sqrt{\frac{2}{5}}c_1^+ & \sqrt{\frac{2}{5}}c_1^- & \sqrt{\frac{2}{5}}c_1^- & -\sqrt{\frac{2}{5}}c_1^+ \\ 0 & \frac{\sqrt{c_1^-}}{5^{1/4}} & -\frac{\sqrt{c_1^+}}{5^{1/4}} & \frac{\sqrt{c_1^+}}{5^{1/4}} & -\frac{\sqrt{c_1^-}}{5^{1/4}} \end{pmatrix}.$$

Each scalar entry multiplies the 2×2 identity. The conjugate momenta transform identically, $(\mathcal{P}_0, \dots, \mathcal{P}_4)^\top = W(\mathbf{p}_1, \dots, \mathbf{p}_5)^\top$.

In these \mathbf{u} -coordinates, the Hamiltonian (11) with coupling constants (13) becomes diagonal:

$$\mathcal{H}_5 = \frac{1}{2\mu}(\mathcal{P}_0^2 + \mathcal{P}_1^2 + \mathcal{P}_2^2 + \mathcal{P}_3^2 + \mathcal{P}_4^2) + \frac{1}{2}\mu\omega^2(u_1^2 + u_2^2 + 4(u_3^2 + u_4^2)), \quad (22)$$

where \mathbf{u}_0 represents the center-of-mass mode and the pairs $(\mathbf{u}_1, \mathbf{u}_2)$ and $(\mathbf{u}_3, \mathbf{u}_4)$ span the two doubly degenerate internal frequency branches.

A.2.1 Trajectories in the center-of-mass frame

For the Hamiltonian (11) with coupling constants (13), using the symmetry-adapted combinations

$$\mathbf{r}_{i+1, i-1}^+ = \mathbf{r}_{i+1} + \mathbf{r}_{i-1}, \quad \mathbf{r}_{i+2, i-2}^+ = \mathbf{r}_{i+2} + \mathbf{r}_{i-2},$$

(with all indices modulo 5) and the constants

$$c_1^\pm = \frac{1}{4}(\sqrt{5} \pm 1),$$

the general trajectories in the center-of-mass frame take the form

$$\begin{aligned} \mathbf{r}_i(t) = & \frac{2}{5} \left[\mathbf{r}_i(0) + c_1^+ \mathbf{r}_{i+1, i-1}^+(0) - c_1^- \mathbf{r}_{i+2, i-2}^+(0) \right] \cos(\omega t) \\ & + \frac{2}{5} \left[\mathbf{r}_i(0) - c_1^- \mathbf{r}_{i+1, i-1}^+(0) + c_1^+ \mathbf{r}_{i+2, i-2}^+(0) \right] \cos(2\omega t) \\ & + \frac{2}{5\mu\omega} \left[\mathbf{p}_i(0) + c_1^+ \mathbf{p}_{i+1, i-1}^+(0) - c_1^- \mathbf{p}_{i+2, i-2}^+(0) \right] \sin(\omega t) \\ & + \frac{1}{5\mu\omega} \left[\mathbf{p}_i(0) - c_1^- \mathbf{p}_{i+1, i-1}^+(0) + c_1^+ \mathbf{p}_{i+2, i-2}^+(0) \right] \sin(2\omega t). \end{aligned} \quad (23)$$

$i = 1, 2, 3, 4, 5$. This describes a superposition of a fundamental mode of frequency $\Omega_1 = \omega$ and its second harmonic $\Omega_2 = 2\omega$. For this coupling choice the relative dynamics is fully resonant, hence periodic.

For $n = 4$, the internal motion is carried by a single D_4 doublet (together with the Nyquist mode when it is excited). Generic initial phases in the doublet produce a (2+2) dimer split, while a distinguished quadrature phase-locking yields a genuine four-body choreography (Section 4.3.1). When the Nyquist mode is also active, C_4 phase matching imposes the additional 1:2 locking that selects the limaçon family discussed in Section 4.1.

By contrast, for $n = 5$ there is no symmetry-protected lower-order choreography: dimers are symmetry-forbidden and any fragmented motion requires additional resonance and phase-matching constraints. In particular, a full five-body choreography exists only at the special resonance $\Omega_2 = 2\Omega_1$.

A.3 Case $n = 6$

We now turn to the six-body case $n = 6$, for which the internal dynamics decomposes into three inequivalent symmetry sectors: two real cosine-sine sectors corresponding to the Fourier labels $\ell = 1, 2$, and the Nyquist sector $\ell = 3$. The associated normal-mode frequencies Ω_ℓ are determined by the three independent coupling constants $\kappa_1^{(6)}, \kappa_2^{(6)}, \kappa_3^{(6)}$ through relation (16) in the main text.

To make this decomposition explicit, introduce the real symmetry-adapted orthonormal coordinates associated with the six particle labels. Let

$$\theta_j := \frac{2\pi}{6}(j-1), \quad j = 1, \dots, 6,$$

and define

$$\begin{aligned} \mathbf{u}_0 &:= \frac{1}{\sqrt{6}} \sum_{j=1}^6 \mathbf{r}_j, \\ \mathbf{u}_{c\ell} &:= \sqrt{\frac{1}{3}} \sum_{j=1}^6 \mathbf{r}_j \cos(\ell\theta_j), & \mathbf{u}_{s\ell} &:= \sqrt{\frac{1}{3}} \sum_{j=1}^6 \mathbf{r}_j \sin(\ell\theta_j), & \ell &= 1, 2, \\ \mathbf{u}_{c3} &:= \frac{1}{\sqrt{6}} \sum_{j=1}^6 (-1)^{j-1} \mathbf{r}_j. \end{aligned}$$

In the center-of-mass frame used throughout the paper,

$$\mathbf{u}_0 \equiv 0.$$

These real variables are the cosine-sine form of the label-Fourier decomposition. After identifying the plane with \mathbb{C} , let

$$u_{c\ell}, u_{s\ell}, u_{c3} \in \mathbb{C}$$

denote the complex representatives of

$$\mathbf{u}_{c\ell}, \mathbf{u}_{s\ell}, \mathbf{u}_{c3} \in \mathbb{R}^2.$$

Then the corresponding label-Fourier coefficients are

$$U_\ell = \frac{1}{\sqrt{2}}(u_{c\ell} - i u_{s\ell}), \quad U_{6-\ell} = \frac{1}{\sqrt{2}}(u_{c\ell} + i u_{s\ell}), \quad \ell = 1, 2,$$

while the Nyquist sector is represented by

$$U_3 = u_{c3}.$$

Here no conjugacy relation between U_ℓ and $U_{6-\ell}$ is implied: after the planar identification $\mathbb{R}^2 \simeq \mathbb{C}$, these are complex planar coefficients. The pair $(U_\ell, U_{6-\ell})$ is simply the complex label-Fourier representation of the real cosine-sine doublet $(\mathbf{u}_{c\ell}, \mathbf{u}_{s\ell})$.

In these variables, the Hamiltonian (15) becomes

$$\mathcal{H}_6 = \frac{1}{2\mu} \sum_{\alpha} \mathbf{P}_{\alpha}^2 + \frac{1}{2} \mu [\Omega_1^2 (\mathbf{u}_{c1}^2 + \mathbf{u}_{s1}^2) + \Omega_2^2 (\mathbf{u}_{c2}^2 + \mathbf{u}_{s2}^2) + \Omega_3^2 \mathbf{u}_{c3}^2],$$

where

$$\alpha = 0, c1, s1, c2, s2, c3, \quad \mathbf{P}_{\alpha} := \mu \dot{\mathbf{u}}_{\alpha}.$$

Hence the internal motion is a superposition of two planar oscillator doublets

$$(\mathbf{u}_{c\ell}, \mathbf{u}_{s\ell}), \quad \ell = 1, 2,$$

together with the Nyquist coordinate \mathbf{u}_{c3} .

The corresponding solutions are

$$\mathbf{u}_{c\ell}(t) = \mathbf{A}_{c\ell} \cos(\Omega_{\ell} t) + \frac{\mathbf{B}_{c\ell}}{\mu \Omega_{\ell}} \sin(\Omega_{\ell} t), \quad \mathbf{u}_{s\ell}(t) = \mathbf{A}_{s\ell} \cos(\Omega_{\ell} t) + \frac{\mathbf{B}_{s\ell}}{\mu \Omega_{\ell}} \sin(\Omega_{\ell} t), \quad \ell = 1, 2,$$

and

$$\mathbf{u}_{c3}(t) = \mathbf{A}_3 \cos(\Omega_3 t) + \frac{\mathbf{B}_3}{\mu \Omega_3} \sin(\Omega_3 t),$$

where

$$\mathbf{A}_{c\ell} = \mathbf{u}_{c\ell}(0), \quad \mathbf{B}_{c\ell} = \mathbf{P}_{c\ell}(0), \quad \mathbf{A}_{s\ell} = \mathbf{u}_{s\ell}(0), \quad \mathbf{B}_{s\ell} = \mathbf{P}_{s\ell}(0),$$

and

$$\mathbf{A}_3 = \mathbf{u}_{c3}(0), \quad \mathbf{B}_3 = \mathbf{P}_{c3}(0).$$

Reconstruction of the real-space trajectories gives

$$\mathbf{r}_i(t) = \sqrt{\frac{1}{3}} \sum_{\ell=1}^2 \left[\mathbf{u}_{c\ell}(t) \cos(\ell\theta_i) + \mathbf{u}_{s\ell}(t) \sin(\ell\theta_i) \right] + \frac{(-1)^{i-1}}{\sqrt{6}} \mathbf{u}_{c3}(t), \quad i = 1, \dots, 6.$$

Equivalently,

$$\begin{aligned} \mathbf{r}_i(t) = & \sqrt{\frac{1}{3}} \sum_{\ell=1}^2 \left[\left(\mathbf{A}_{c\ell} \cos(\Omega_\ell t) + \frac{\mathbf{B}_{c\ell}}{\mu\Omega_\ell} \sin(\Omega_\ell t) \right) \cos(\ell\theta_i) \right. \\ & \left. + \left(\mathbf{A}_{s\ell} \cos(\Omega_\ell t) + \frac{\mathbf{B}_{s\ell}}{\mu\Omega_\ell} \sin(\Omega_\ell t) \right) \sin(\ell\theta_i) \right] \\ & + \frac{(-1)^{i-1}}{\sqrt{6}} \left(\mathbf{A}_3 \cos(\Omega_3 t) + \frac{\mathbf{B}_3}{\mu\Omega_3} \sin(\Omega_3 t) \right). \end{aligned}$$

This is precisely the $n = 6$ specialization of the inverse Fourier reconstruction (4), written in real cosine-sine coordinates. The traveling-wave Fourier class used in Theorem 2 is obtained by imposing the corresponding one-sided condition on the complex label-Fourier coefficients.

A.4 General $n > 6$

For a general quadratic D_n -invariant system with $n > 6$, the internal dynamics admits a real symmetry-adapted normal-mode decomposition obtained from the discrete Fourier transform. In the center-of-mass frame we set

$$\mathbf{u}_0 := \frac{1}{\sqrt{n}} \sum_{i=1}^n \mathbf{r}_i, \quad \mathbf{u}_0 \equiv 0.$$

For

$$q_\ell := \frac{2\pi\ell}{n}, \quad \ell = 1, \dots, \left\lfloor \frac{n-1}{2} \right\rfloor,$$

define the cosine-sine coordinates

$$\mathbf{u}_{c\ell} = \sqrt{\frac{2}{n}} \sum_{i=1}^n \mathbf{r}_i \cos(q_\ell(i-1)), \quad \mathbf{u}_{s\ell} = \sqrt{\frac{2}{n}} \sum_{i=1}^n \mathbf{r}_i \sin(q_\ell(i-1)).$$

For even n , there is in addition the Nyquist coordinate

$$\mathbf{u}_{Ny} = \frac{1}{\sqrt{n}} \sum_{i=1}^n (-1)^{i-1} \mathbf{r}_i.$$

These variables are the real cosine-sine form of the label-Fourier coefficients appearing in Theorem 2. After identifying the plane with \mathbb{C} , let

$$u_{c\ell}, u_{s\ell}, u_{Ny} \in \mathbb{C}$$

denote the complex representatives of

$$\mathbf{u}_{c\ell}, \mathbf{u}_{s\ell}, \mathbf{u}_{Ny} \in \mathbb{R}^2.$$

Then the corresponding label-Fourier coefficients are

$$U_\ell = \frac{1}{\sqrt{2}}(u_{c\ell} - i u_{s\ell}), \quad U_{n-\ell} = \frac{1}{\sqrt{2}}(u_{c\ell} + i u_{s\ell}), \quad \ell = 1, \dots, \left\lfloor \frac{n-1}{2} \right\rfloor,$$

while for even n the Nyquist sector is represented by

$$U_{n/2} = u_{Ny}.$$

No conjugacy relation between U_ℓ and $U_{n-\ell}$ is implied in this complex planar notation. The pair $(U_\ell, U_{n-\ell})$ is the label-Fourier representation of the real cosine-sine doublet $(\mathbf{u}_{c\ell}, \mathbf{u}_{s\ell})$.

In these coordinates the quadratic Hamiltonian separates into independent planar oscillators. For each ℓ ,

$$\ddot{\mathbf{u}}_{c\ell} + \Omega_\ell^2 \mathbf{u}_{c\ell} = 0, \quad \ddot{\mathbf{u}}_{s\ell} + \Omega_\ell^2 \mathbf{u}_{s\ell} = 0,$$

and, when present,

$$\ddot{\mathbf{u}}_{Ny} + \Omega_{Ny}^2 \mathbf{u}_{Ny} = 0.$$

Hence

$$\mathbf{u}_{c\ell}(t) = \mathbf{A}_{c\ell} \cos(\Omega_\ell t) + \frac{\mathbf{B}_{c\ell}}{\mu\Omega_\ell} \sin(\Omega_\ell t), \quad \mathbf{u}_{s\ell}(t) = \mathbf{A}_{s\ell} \cos(\Omega_\ell t) + \frac{\mathbf{B}_{s\ell}}{\mu\Omega_\ell} \sin(\Omega_\ell t),$$

and, for even n ,

$$\mathbf{u}_{Ny}(t) = \mathbf{A}_{Ny} \cos(\Omega_{Ny} t) + \frac{\mathbf{B}_{Ny}}{\mu\Omega_{Ny}} \sin(\Omega_{Ny} t).$$

The particle trajectories are reconstructed as

$$\mathbf{r}_i(t) = \sqrt{\frac{2}{n}} \sum_{\ell=1}^{\lfloor (n-1)/2 \rfloor} \left[\mathbf{u}_{c\ell}(t) \cos(q_\ell(i-1)) + \mathbf{u}_{s\ell}(t) \sin(q_\ell(i-1)) \right], \quad i = 1, \dots, n,$$

with the additional Nyquist contribution, for even n ,

$$\mathbf{r}_i(t) \mapsto \mathbf{r}_i(t) + \frac{(-1)^{i-1}}{\sqrt{n}} \mathbf{u}_{Ny}(t).$$

Thus the real normal-coordinate formulation used in the appendices is the cosine-sine realization of the sector decomposition used in Theorem 2: each pair

$$(\mathbf{u}_{c\ell}, \mathbf{u}_{s\ell})$$

represents one non-self-conjugate label-Fourier sector pair $(\ell, n - \ell)$, while for even n the Nyquist sector is represented by the single coordinate \mathbf{u}_{Ny} . The traveling-wave Fourier class is obtained by imposing the corresponding one-sided condition on the complex coefficients U_ℓ .